Turkish Journal of Earth Sciences (Turkish J. Earth Sci.), **Vol. 12**, 2003, pp. 175-198. *Copyright ©TÜBİTAK*

Geology and Hydrothermal Alteration of the Aydın-Salavatlı Geothermal Field, Western Anatolia, Turkey

İSMAİL HAKKI KARAMANDERESİ[1] & CAHİT HELVACI[2]

[1] Maden Tetkik ve Arama Genel Müdürlüğü (MTA), Ege Bölge Müdürlüğü, TR-35042 Bornova, İzmir - Turkey

[2] Dokuz Eylül Üniversitesi, Mühendislik Fakültesi, Jeoloji Mühendisliği Bölümü, TR-35100 Bornova, İzmir - Turkey (e-mail: cahit.helvaci@deu.edu.tr)

Abstract: The Aydın-Salavatlı geothermal field is located in the middle part of the Büyük Menderes Graben, and is characterized by normal-fault structures. The stratigraphic sequence of the Aydın-Salavatlı geothermal field consists of metamorphic rocks of the Menderes Massif and sedimentary rocks deposited during the rifting period of the Menderes Massif in the Miocene. Geological data suggest that there is a connection between tectonic development and periods of hydrothermal alteration.

Hydrothermal alteration in the Aydın-Salavatlı geothermal field occurred in five distinct periods, and all are related to different stages of faulting systems, from the Middle Miocene up to the present. The first period of hydrothermal alteration was characterized by mercury and antimony mineralization related to acidic intrusions, and by the occurrence of rutile mineralization within quartz veins. Gabbros and associated dykes developed in the second period. In this period, gneisses were subjected to hydrothermal alteration. The third period was characterized by granite intrusions. Specularite, talc, calcite, quartz, and aragonite mineralization and travertine formed along the margins of these intrusions. The fourth period was marked by albite and chlorite mineralization that developed during N–S faulting. Hydrothermal alteration zones which developed in the last period are associated with active faults along which hot fluid is circulating. These faults have more than 100 m of downthrow, and formed during the final period of graben formation. Hydrothermal alteration products caused by the circulation of geothermal fluids within these faults in Upper Miocene sediments include kaolinite, illite, montmorillonite, dickite, vermiculite, calcite, pyrite, dolomite and hydrobiotite. These minerals are still precipitating/forming in active circulation zones. Thermal waters of the Aydın-Salavatlı geothermal field are a Na-HCO_3 type with high CO_2 and B contents that are associated with metamorphic rocks of the Menderes Massif and hydrothermal alteration which developed via water-rock interactions. Geophysical studies were used to outline tectonic structures and frames of the Salavatlı geothermal field.

Key Words: geothermal field, hydrothermal alteration, Büyük Menderes Graben, Salavatlı, western Anatolia, Turkey

Aydın-Salavatlı Jeotermal Sahasının Jeolojisi ve Hidrotermal Alterasyonu, Batı Anadolu, Türkiye

Özet: Aydın-Salavatlı jeotermal sahası Büyük Menderes vadisi orta bölümünde yer alır ve normal faylı bir yapı ile temsil edilir. Aydın-Salavatlı jeotermal sahası stratigrafik kesiti Menderes Masifi metamorfik kayaları ve bunun üzerine Miyosen'den günümüze kadar devam eden dönemde çökelmiş sedimanter kaya topluluklarından oluşmaktadır. Jeolojik veriler Menderes Masifi'ndeki tektonik gelişim ve evreleri ile hidrotermal alterasyonların ilişkili olduğunu göstermiştir.

Aydın-Salavatlı jeotermal sahasındaki hidrotermal alterasyon beş farklı evreye ayrılmıştır. Bu evreler genleşme tektoniği fayları ile belirlenmiş olup Orta Miyosen'den itibaren günümüze kadar devam etmiştir. İlk evre hidrotermal alterasyon civa ve antimuan mineralleşmesi ve bunlarla ilişkili asidik intrüzyonların yerleşmesidir. Bu evre fosil jeotermal sistemlerde gözlenen mineral parajenezleri, rutil mineralizasyonları ve kuvars çatlak dolguları ile karakterize edilmektedir. Gabro ve onlara eşlik eden dayklar ikinci evreyi oluşturur. Bu evrede gnaysların hidrotermal alterasyona uğradığı belirlenmiştir. Üçüncü evrede ise granit intrüzyonları yerleşmiştir. Bu intrüzyonların yan kayalarında spekülarit, talk, kalsit, kuvars, ve aragonit mineralleri ile üst boşalım bölgelerinde traverten oluşumları görülür. Dördüncü evre albit-klorit mineralizasyonu ile kuzey–güney uzanımlı fay hatlarında belirlenmiştir. Son evre ise yüksek sıcaklıklı jeotermal akışkanın dolaştığı fay zonlarında belirlenmiştir. Bu fay zonlarındaki hareket 100 metreden fazladır ve graben oluşumunu belirleyen son hareketlerdir. Üst Miyosen

tortulları içinde dolaşan jeotermal akışkanlar bu fay zonlarında hidrotermal alterasyona sebep olmuşlardır. Aktif hidrotermal alterasyon mineralojisi kaolinit, illit, montmorillonit, dikit, vermikülit, kalsit, pirit, dolomit ve hidrobiyotit minerallerinden oluşmaktadır. Bu minerallerin varlığı aktif jeotermal akışkan dolaşımının halen sürdüğünü göstermektedir. Aydın-Salavatlı jeotermal sahasının suları, Menderes Masifi kayalarının su-kaya etkileşimi ile gelişen hidrotermal alterasyona bağlı olarak yüksek CO_2 ve B içerikli Na-HCO_3 tipindedir. Jeofizik çalışmaları Salavatlı jeotermal sahasının tektonik yapısını ve konumunu belirlemek için kullanılmıştır.

Anahtar Sözcükler: jeotermal saha, hidrotermal alterasyon, Büyük Menderes Grabeni, Salavatlı, batı Anadolu, Türkiye

Introduction

Extensive tectonic activity, especially the formation of east–west grabens, has dictated the shape of western Anatolia (Figure 1). Of these, Büyük Menderes and Gediz grabens host the main and the most important geothermal fields of Turkey. The distribution of geothermal fields in Turkey closely follows the tectonic patterns. All of the hot springs with temperatures above 50–100ºC in eastern and western Anatolia are clearly related to young volcanic activity and block faulting. Post-collisional volcanic activity, lasting from the Late Miocene to present, has been responsible for heating the geothermal fields (Şimşek 1997; Yılmaz 1997; Demirel & Şentürk 1996). The high thermal activities are reflected in widespread acidic volcanic activity with much hydrothermal alteration, fumaroles, and more than 600 hot springs with temperatures up to 100 ºC (Çağlar 1961).

The Aydın-Salavatlı geothermal field is located in the middle part of the Büyük Menderes Graben, and is characterized by E–W-trending normal faults (Figure 1).

The stratigraphic sequence of the field is composed of metamorphic rocks of the Menderes Massif and overlying the Miocene sedimentary rocks deposited during the Miocene exhumation of the massif. Field data suggest that there is a connection between tectonic development and periods of hydrothermal alteration. Several deep wells were drilled (AS-1, 1510 m and AS-2, 962 m) and revealed low resistivity zones (Karamanderesi 1997).

Preliminary studies were conducted on a regional scale by Karamanderesi (1972). Geochemical analysis of water from hot springs near Salavatlı village indicated that the area has hot-water-dominated geothermal potential, and geophysical studies outlined the structural situation of the geothermal field. Geophysical studies using gravity (Gülay 1988) and electrical resistivity methods (Şahin 1985) indicated that the geothermal field is located along fault systems near the towns of Salavatlı and Sultanhisar.

A couple of deep wells were drilled by General Directorate of Mineral Research and Exploration (MTA) (AS-1, 1510 m below ground level; and AS-2, 962 m, Figure 2) within a low resistivity zone (5–10 ohmm) outlined by resistivity-depth sounding studies. Cuttings from the AS-1 and AS-2 wells near Salavatlı were studied by petrographic microscopy and XRD methods, and the nature and distribution of their mineral parageneses were determined. The data obtained from the drill cores of these wells are the subject of this paper, and are used to explain a model for the geothermal system of the Aydın-Salavatlı field.

Materials and Methods

Relatively detailed cutting analyses along with various other borehole logs were used to assess the geothermal system into which wells AS-1 and AS-2 were drilled. During drilling, rock cuttings were taken every 2 m and were properly labelled. Circulation losses and rates of penetration were recorded for each drill pipe sunk.

Temperature logs were carried out during drilling to locate aquifers and assess the condition of the wells. The temperature-logging equipment comprised Amerada logging tools. These logs provide important information on temperature conditions, flow paths and feed-zones in geothermal systems. Temperature logs have also been prepared after drilling and production.

The well-testing method was controlled by lip-pressure measurements that give total mass-flow rate and the heat content (enthalpy) of a two-phase geothermal fluid from a discharge pipe.

Samples in the well or drill boxes are wettened by pouring water onto them. Wetting the cuttings is necessary to enhance the visibility of the samples or

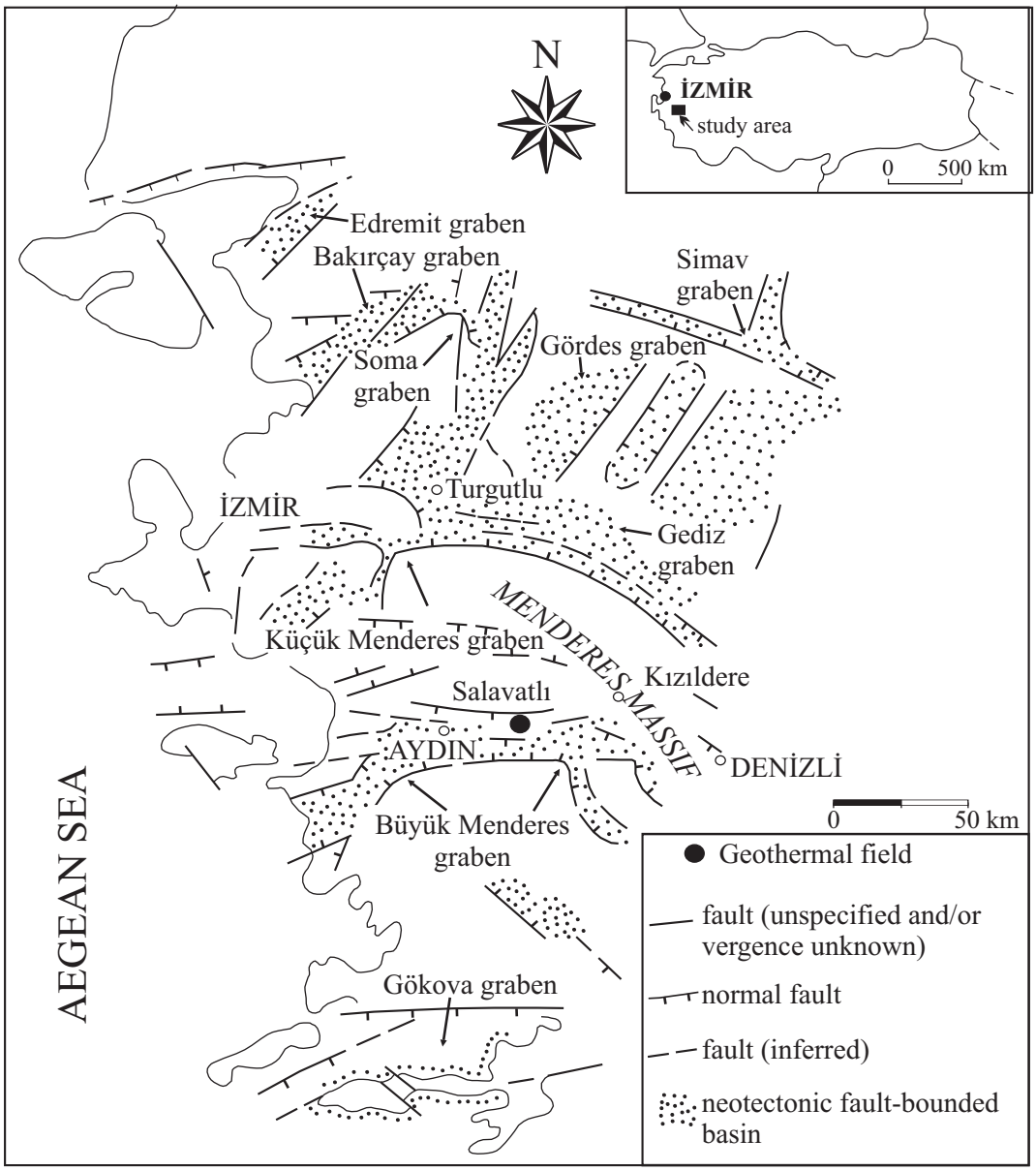

Figure 1. Main tectonic features of western Anatolia and location map of the Aydın-Salavatlı geothermal field.

certain features such as finely disseminated sulphides (e.g., pyrite). The wet samples were then placed onto the mounting stage of the microscope for investigation. Cutting examination was done using binocular microscope with a 5x10 magnification of the field of study. Initial information obtained includes stratigraphic/ sedimentological features, alteration mineralogy and evidence of permeabilities. In addition to binocular microscopic study, thin sections for petrographic study were made in order to expand or confirm preliminary findings from the cuttings. However, this method intends to complement rather than replace careful binocular microscopic studies and adds understanding with regard to rock-mineral deposition and alteration. Selected thin-section samples were analysed using the petrographic microscope.

X-ray diffractometric analyses were done on the ~4 μm fractions of particular samples from the cuttings in

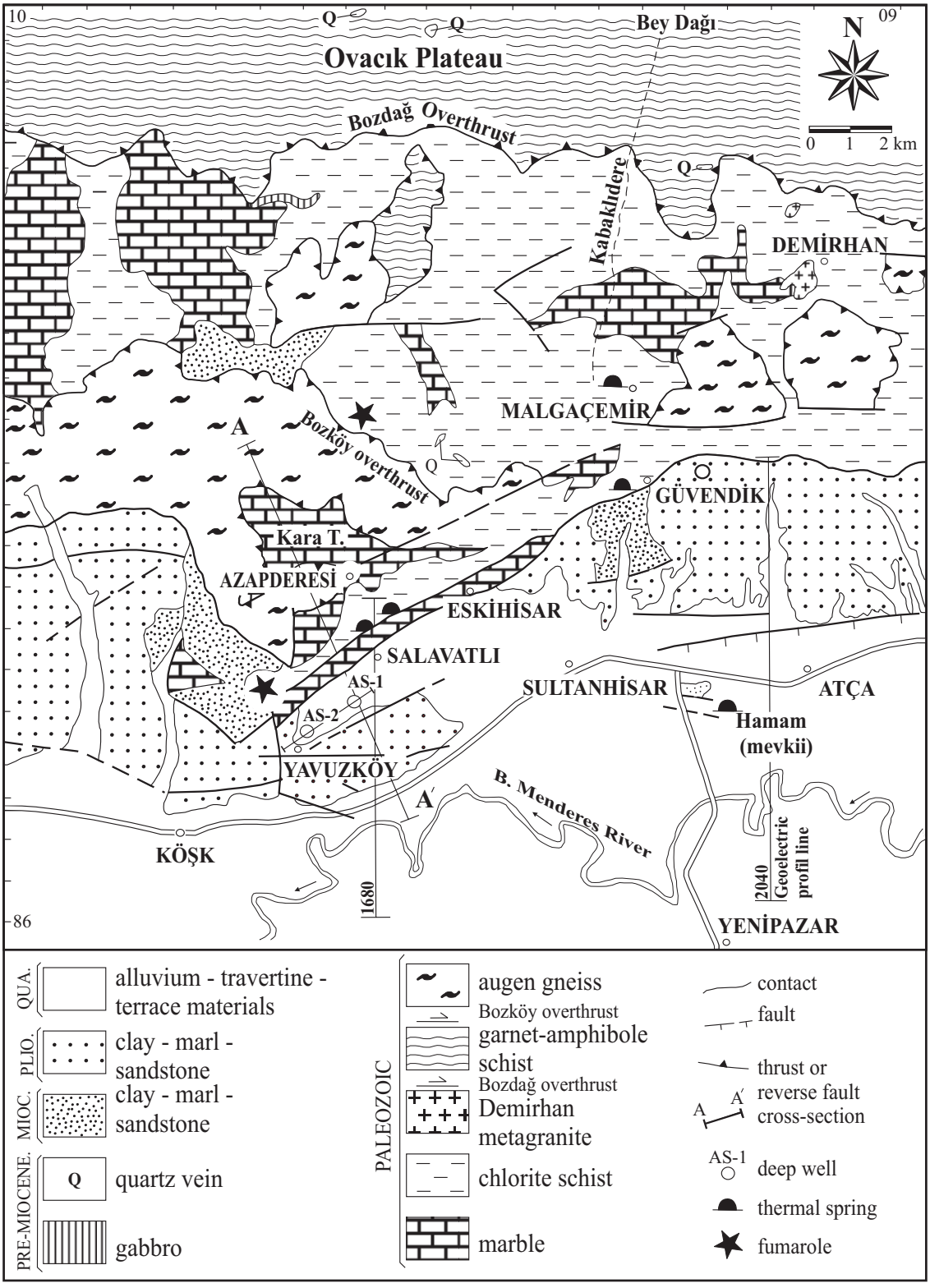

Figure 2. Geological map of the Aydın-Salvatlı geothermal field.

order to confirm and identify the types of clay minerals present in the cuttings. Approximately two teaspoons of drill cuttings were placed into a test tube, and dust was washed out with distilled water. The tubes were filled 2/3 full with distilled water and plugged with rubber stoppers. The tubes were placed in a mechanical shaker for 4–8 hours, depending on the alteration grade of the samples. The contents were allowed to settle for 1–2 hours until only particles finer than approximately 4 microns were left in suspension. A few millilitres of liquid was pipetted from each tube and about 10 drops placed on a labelled glass plate. An effort was made to avoid thick samples. A duplicate was made of each sample and left to dry at room temperature overnight. One set of samples was placed in a desiccator containing glycol ($C_2O_6O_2$) solution and the other into a desiccator containing $CaCl_2 2H_2O$. The samples were stored at room temperature for at least 24 hours. Thick samples needed a longer time in the desiccator – at least 48 hours. Both sets of samples were run from 2 to 15° on the XRD. One set of the samples (normally the glycolated one) was placed on an asbestos plate and heated in a preheated oven at 550–600 °C. The oven temperature did not exceed 600 °C. The exact location on the asbestos of individual samples was established before heating because labelling disappears during the heating process. The samples were cooled sufficiently before further treatment. Then the samples were run from 2 to 15° on the XRD.

Geologic Setting of the Menderes Massif

The Menderes Massif is a crustal-scale (covering more than 40,000 km^2), elongate (with its long axis trending NE–SW) metamorphic core complex in western Turkey (Figure 1). It is structurally overlain by the Lycian Nappes (e.g., Graciansky 1972; Collins & Robertson 1997, 1999; Oberhänsli *et al.* 2001) in the south and rocks of the İzmir-Ankara Neotethyan suture (e.g., Şengör & Yılmaz 1981; Okay & Siyako 1993; Okay *et al.* 1996a) in the north. There are claims that the massif can be correlated with the Cycladic Massif in the Aegean (Dürr *et al.* 1978; Oberhänsli *et al.* 1998); but others argue that these massifs do not represent mutually lateral continuations (e.g., Ring *et al.* 1999; Okay 2001).

The massif forms one of the most important geological entities of the Turkish Alpine orogenic belt in western Turkey, and has been under the influence of N–S crustal extensional tectonics since the Early Miocene (e.g., Koçyiğit *et al.* 1999; Bozkurt 2001a, b; Bozkurt & Oberhänsli 2001a, b; Seyitoğlu *et al.* 2002; Sözbilir 2002). It is dissected into northern, central and southern submassifs along the E–W-trending seismically active Gediz and Büyük Menderes grabens, respectively; the grabens are the result of N–S extension which commenced by the Early Pliocene (~5 Ma) (e.g., Koçyiğit *et al.* 1999; Bozkurt 2000, 2001a, 2002; Sarıca 2000; Yılmaz *et al.* 2000; Genç *et al.* 2001; Gürer *et al.* 2001; Sözbilir 2001, 2002; Yılmaz & Karacık 2001). It is now agreed that each submassif represents a core complex formation in the footwall of presently low-angle normal faults, but their exhumations have occurred at different times (e.g., Bozkurt & Park 1994, 1997a, b; Verge 1995; Hetzel *et al.* 1995a, b, 1998; Okay *et al.* 1996b; Koçyiğit *et al.* 1999; Bozkurt & Satır 2000; Bozkurt 2001b; Gessner *et al.* 2001a, b; Gökten *et al.* 2001; Işık & Tekeli 2001; Sözbilir 2001).

The Menderes Massif is traditionally described as a thick lithologic succession made up of: (1) a '*core*' consisting mostly of granitic augen gneiss with boundinaged layers of metagabbros – they show granulite and eclogite relics and, (2) a '*cover*' series of low-grade metasediments comprising metapelites with subordinate psammite, amphibolite and marble intercalations (Palaeozoic *'schist cover'*) and a marble-dominated sequence (Mesozoic-Cenozoic '*marble cover*') containing emery, metabauxite, and rudist fossils. The age of the granitic protolith for the augen gneisses is assigned as Late Precambrian and Early Cambrian (c. 521–572 Ma, averaging 550 Ma: U-Pb and Pb-Pb single zircon evaporation methods) (e.g., Hetzel & Reischmann 1996; Loos & Reischmann 1999; Gessner *et al.* 2001a). Fossil evidence indicates a Permian to Middle Palaeocene age for the cover rocks (e.g., Phillipson 1918; Önay 1949; Çağlayan *et al.* 1980; Konak *et al.* 1987). The readers are referred to Okay (2001, 2002), Özer *et al.* (2001) and Güngör & Erdoğan (2002) for further reading.

The contact relationship between the so-called '*core*' and '*cover*' rocks is still debated. The views fall into three major categories: (1) the contact is a major unconformity called the supra Pan-African unconformity (Şengör *et al.* 1984); (2) it is a south-facing extensional shear zone with preserved local igneous contacts along which the core rocks are intrusive into cover rocks (Bozkurt *et al.* 1993,

1995; Bozkurt & Park 1994, 1997a, b, 1999; Hetzel & Reischmann 1996; Bozkurt & Satır 2000; Lips *et al.* 2001). These authors suggest that the so-called core rocks have been exhumed in the footwall of this shear zone during a top-to-the-SSW deformation; (3) while others confirm the tectonic nature of this contact but claim that it is south-facing thrust fault with a top-to-the-south deformation (Ring *et al.* 1999; Gessner *et al.* 2001a).

The literature suggests that the core rocks have been affected by granulite facies metamorphism followed by an eclogite facies event, then by an amphibolite facies metamorphic overprint (Candan 1995, 1996; Candan *et al.* 1997, 2001; Oberhänsli *et al.* 1997; Candan & Dora 1998). The lack of eclogite and granulite relicts in the augen gneisses suggests that these rocks were affected only by the latest amphibolite-facies metamorphism (e.g., Candan *et al.* 2001 and references therein).

The most agreed-upon concept concerning the Menderes Massif is that the massif has acquired its massif character during an Alpine regional HT/MP Barrovian-type tectono-metamorphic event termed "main Menderes metamorphism (MMM)" during Eocene (Rb-Sr mica ages of 35±5 Ma, Satır & Friedrichsen 1986 and 62–43 Ma, Bozkurt & Satır 2000; ^{40}Ar-^{39}Ar mica age of 43–37 Ma, Hetzel & Reischmann 1996; and ^{40}Ar-^{39}Ar laser probe mica age of 36±2, Lips *et al.* 2001). It is suggested that the MMM was a result of the burial of the massif area beneath the southward moving Lycian nappes – rooted from the İzmir-Ankara Neotethyan suture zone, thus causing regional metamorphism and deformation of the massif (Şengör & Yılmaz 1981; Şengör *et al.* 1984). On the other hand, the existing structures formed during the MMM indicate a top-to-the-NNE tectonic transport (Bozkurt 1995; Hetzel *et al.* 1998; Bozkurt & Park 1999; Bozkurt 2001b; Bozkurt & Oberhänsli 2001a). Temperatures during the 'MMM' reached ~550 °C while pressure is estimated as ≤5 kbar (Whitney & Bozkurt 2002). Subsequent exhumation occurred along originally high-angle but presently low-angle normal faults during Miocene time (e.g., Bozkurt & Park 1994, 1997a, b; Hetzel *et al.* 1995a, b, 1998; Verge 1995; Hetzel & Reischmann 1996; Koçyiğit *et al.* 1999; Bozkurt 2000, 2001a, b; Gessner *et al.* 2001a, b; Gökten *et al.* 2001; Işık & Tekeli 2001; Lips *et al.* 2001; Bozkurt & Oberhänsli 2001a; Sözbilir 2001, 2002; Seyitoğlu *et al.* 2002).

Western Anatolia is characterized by a number of approximately east–west-trending, subparallel, normal fault zones bordering a set of grabens and intervening horst blocks. Seismic activity is intense and has been recorded by a network of instruments roughly encircling the active faults. Motions on the faults confirm that extension is in a north–south direction. Western Anatolia and the Aegean regions have long been known to represent a broad zone of extension (Phillipson 1918), stretching from Bulgaria in the north to the Aegean arc in the south (McKenzie 1972).

There are about ten ~E–W-oriented grabens in western Anatolia. The best-developed grabens are Büyük Menderes, Gediz, Edremit, Gökova and Bergama. They are c. 100–150-km long and 5–15-km wide. In each graben, one margin is characterized by steeper topography, associated with surface breaks. On the footwall margins of the grabens, planar faults are readily observed (Figure 1).

N–S extensional tectonics in the Aegean region have been explained by "tectonic escape" (Şengör 1979, 1980, 1982, 1987; Dewey *et al.* 1979; Şengör *et al.* 1985) or "back-arc spreading" (Le Pichon & Angelier 1979, 1981; McKenzie 1978; Jackson & McKenzie 1988; Melenkamp *et al.* 1988). These models and their variations (Şengör 1987; Dewey 1988) indicate the timing of initiation of extensional tectonics as Tortonian (Late Miocene) and/or younger. According to Seyitoğlu & Scott (1991, 1992), the palynological ages from the E–W-trending Büyük Menderes Graben show that in western Turkey, the N–S extensional tectonics had begun during latest Oligocene–Early Miocene. The fact that the Late Miocene and Plio-Quaternary tectonic evolution of this region is of the extensional nature and still active is also demonstrated by seismic studies. Eyidoğan (1988) reported extension of 13.5 mm/yr based on seismicity over the last 40 years. Volcanic activity, whose increase coincided with the neotectonic phase, was studied in detail by Ercan *et al.* (1985).

Geophysical studies and drilling have shown a normal fault structure, resulting in stepwise graben formation, which is also characteristic of the Germencik, Salavatlı, and Kızıldere geothermal fields in the Büyük Menderes Graben (Figure 1). For further information the reader is referrred to Konak *et al.* (1987) and Dora *et al.* (1992). Broad E–W-striking normal graben faults cut across nearly 100-m-thick cataclasites, which were formed at

the base of detachment faults, and non-metamorphic Neogene sediments on the crystalline basement (Hetzel *et al.* 1995b). Several intermediate to basic volcanic extrusions and geothermal springs in the central parts of the Menderes Massif are directly related to the graben system. Early fossil geothermal systems developed along tectonic zones during the dome-forming period. The development and evolution of these systems are related to neotectonic activity (Figure 2).

Although the Menderes Massif has been the subject of intense research since 1990s there are still many problems concerning the lithology, age, structure, deformation and metamorphism of the Menderes Massif. We therefore suggest that readers refer to Bozkurt & Oberhänsli (2001a, b) for further reading.

Geology of the Aydın-Salavatlı Area

The Aydın-Salavatlı geothermal field is located in the north-central part of the Büyük Menderes Graben, and covers an area about 8 km long and 2 km wide (Figure 2). The geological sequence of this area includes orthogneiss and paragneiss, fine-grained schists, coarse-grained augen gneiss, mica schist, quartz schist, metaquartzite and marble units. Structural analysis shows that these units have been reverse-faulted and that the gneisses have been thrusted over the schists and marbles. These structures can be seen at the surface (Akartuna 1965) and also in the cross-section between the AS-1 and AS-2 wells (Figures 3 & 4).

Tertiary sedimentary rocks, which have been filling the graben that developed as result of neotectonic activity, have been deposited over the metamorphic basement. These Neogene sedimentary rocks include coarse- and fine-grained sandstones, siltstones, and well-cemented conglomerates, and are separated by a thin lignite layer at the base of the sequence. Sediments thicker than 1000 m have been drilled through in the Büyük Menderes Graben at the Germencik-Ömerbeyli geothermal field (Karamanderesi *et al.* 1987). Travertine deposits, precipitated from cold or hot springs along the faults, are present locally. Hot springs having 32°C temperatures near Malgaçemir village are evidence of present geothermal activity.

Based upon their mineral parageneses (Table 1), metamorphic rocks of the Menderes Massif are known to be the products of regional metamorphism characterized by medium to high temperature and pressure. A mineral paragenesis including chlorite - biotite - muscovite - garnet - staurolite - kyanite - sillimanite occurs within allochthonous augen gneisses and cover schists.

Observations within the massif show that large fissures and fracture zones developed during neotectonic activity, and quartz veins and calcite and chlorite veins occur in swarms related to deep-seated intrusive bodies.

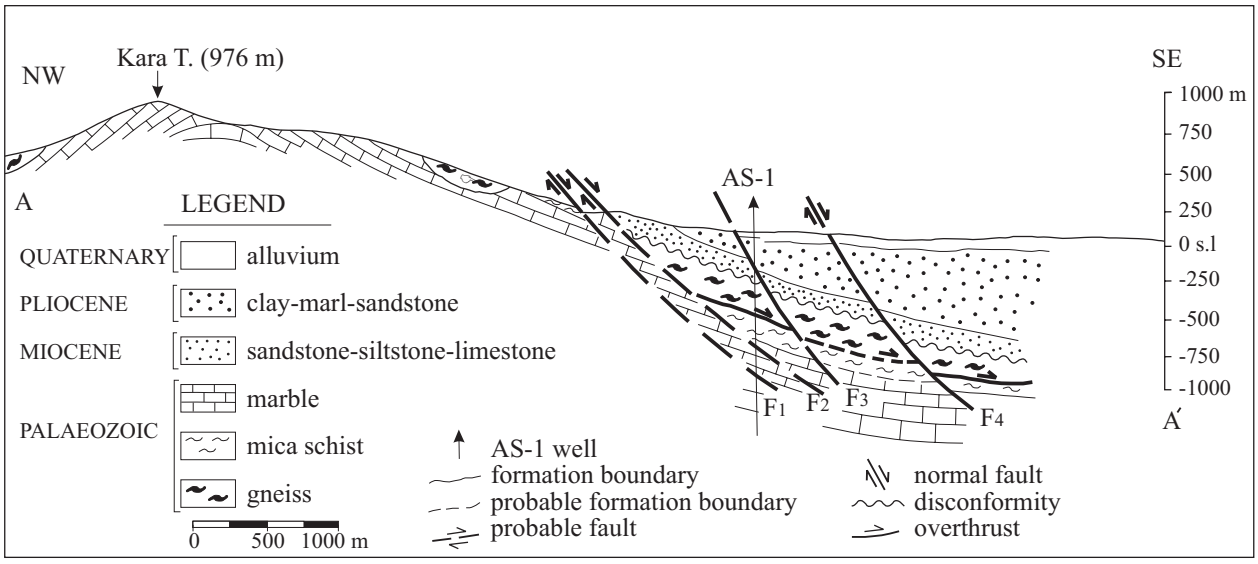

Figure 3. Geological cross-section of the Aydın-Salavatlı geothermal field (see Figure 2 for location).

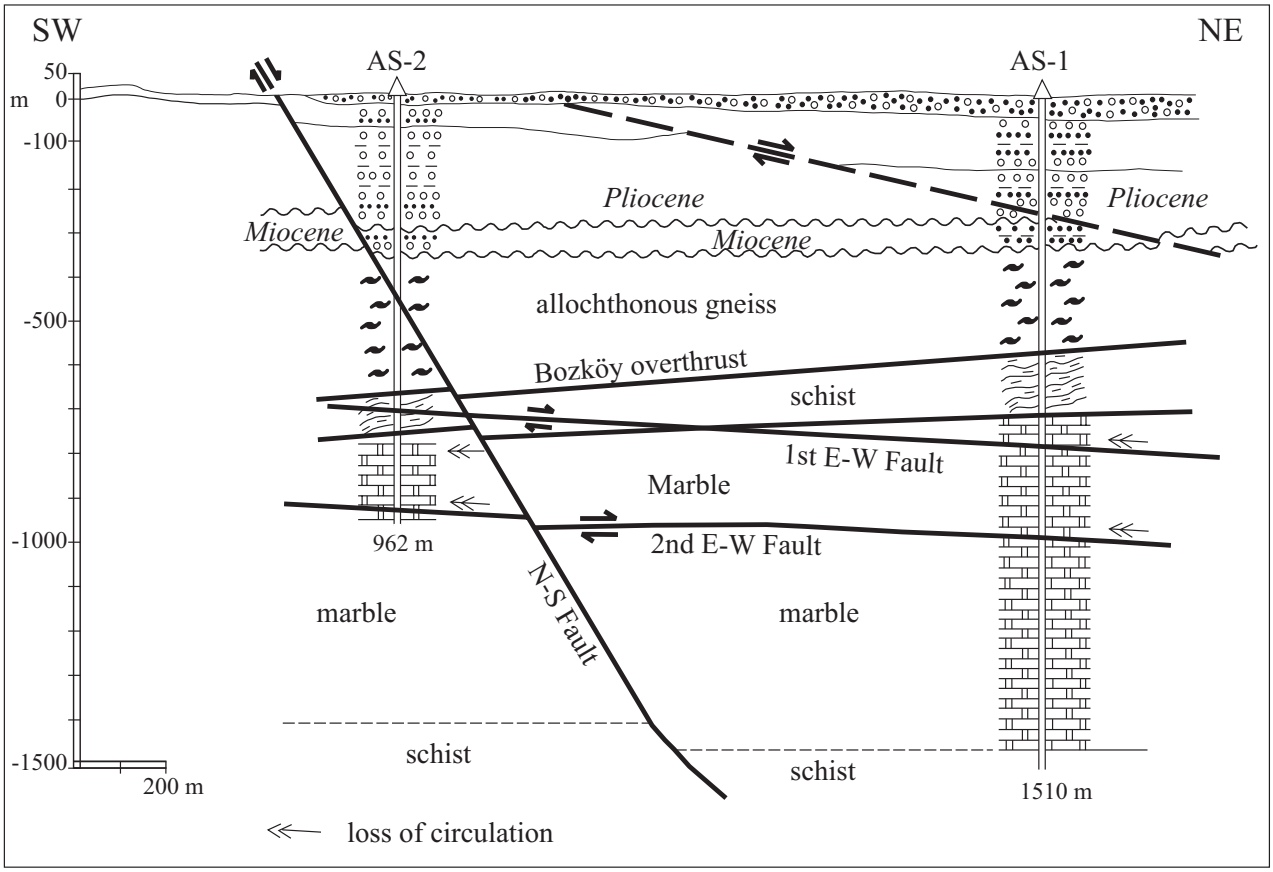

Figure 4. Cross-section through the Aydın-Salavatlı geothermal field (see Figure 2 for location).

These intrusives are not exposed because of the greater depths of their magma chambers, but a few outcrops bearing rutile, titanite, limonite, quartz, calcite and siderite can be observed in the Ovacık plateau at the northern end of the study area (Figure 2). The erosion surfaces of these outcrops have altitudes of 900 m.

From the Ovacık plateau toward the south at lower altitudes, dykes of gabbro and its derivatives, which have intruded along small-scale fracture zones and cooled during the Quaternary, are present. Silicified zones have developed along the margins of these dykes. The mineralogical composition of the gabbroic intrusive rocks (of Early Miocene age [or post-metamorphic]) is as follows: plagioclase, clinopyroxene, orthopyroxene, olivine, biotite, uralite, zoisite, chlorite, apatite, magnetite and garnet. Locally, these gabbroic rocks have schistose textures. Where erosion has been slow, travertine deposits are present along the margins of these silicified zones at the altitudes of the regional discharge zones. Fracture-related mineralization includes epidote, pyrite, arsenopyrite, garnet and clay minerals. An example of such an outcrop is at the Kabaklıdere locality. Toward the south, a similar sort of activity is present within the vicinity of Malgaçemir and Azapderesi. The gabbro intrusion exposed near Malgaçemir village continues to be a heat source (Figure 2).

Travertine deposits along fossil discharge areas are at an altitude of 550 m due to regional neotectonic uplift. Quartz veins and travertine deposits are exposed at a discharge altitude of 600 m in Azapderesi village. Quartz veins facilitated the development of alteration zones of dolomite, calcite, quartz, and clay along fracture zones within the host rock.

The fault systems, clearly traceable around Salavatlı, Eskihisar and Güvendik villages where regional neotectonic activity continues, are imprints of partially

Table 1. Mineral paragenesis of surface samples and well cuttings in the Aydın-Salavatlı geothermal field.

Mineral	Regional metamorphic or relict, from igneous and/or sedimentary mineral assemblages	Metasomatic or early hydrothermal stage	Active hydrothermal stage
oligoclase	———		
andesine	———	———	
albite		———	———
sillimanite	———		
biotite	———	———	
muscovite	———	———	
garnet*	——— (1st)	——— (2nd)	
tourmaline*	——— (1st)	——— (2nd)	———
apatite	———	———	———
epidote		———	———
zircon	———	———	
pyrite		———	———
siderite		———	———
dolomite		———	———
calcite	———	———	———
vermiculite		———	———
hydrobiotite		———	———
quartz	———	———	———
illite		———	———
kaolinite		———	———
dickite		———	———
montmorillonite		———	———
chlorite	———	———	———
opaque mineral(s)	———	———	———

* _ Two different stages of mineral crystallisation.

cooled intrusives. Vein mineralization of calcite, quartz, gypsum, sulphur, pyrite and clay occurs along these faults. It has been observed that travertine and travertine-sulphur deposits are located in NE–SW- and N–S-trending fault zones, respectively (Figure 2). The N–S-trending faults can be correlated with cross-faults described by Şengör (1987), and are illustrated in Figures 2 and 4.

Sulphur efflorescence related to the fracture zones is exposed at a 100-m altitude to the east of Salavatlı village, and sulphur deposits with travertine are exposed at the same altitude at Güvendik village. At an altitude of 50 m, calcite, quartz, clay and sulphur efflorescence occur between Sultanhisar and Atça (Figure 2). Sulphur efflorescence, clays, gypsum and small-scale carbonate mineralization are surface geothermal manifestations along these faults.

The chemical composition of geothermal waters is shown in Table 3. The reservoir temperature, with respect to the chemical composition given in Table 3, has been stated to be 160–175°C according to the method of Giggenbach (1986). Also, the values of two deep well temperatures were measured with Amerada logging tools as 169.77–175.62°C (Tables 4 & 5). The chemistry of the waters was determined to be of the Na-K bicarbonate type. Naturally, it is necessary to determine the chemistry of the encrustation that will develop from these sorts of waters, which, in this case, precipitate calcite and illite. Water samples were taken from the total discharge of the wells thrown out into the atmosphere. Total discharge was measured from the well, which had been opened for a vertical production test. Total discharge data are as follows WHP (bar) 2.27; Patm: 14.6 psi.a; 11% steam, 297 t of water; 39.8 t of steam. Total production was calculated at 336.8 t/h.

The mineralized zones observed along the N–S traverse, as mentioned above, are related to E–W fault systems which become younger toward the south. This type of structure can be observed clearly in the NW–SE cross-section (Figure 3). There are two N–S-trending strike-slip faults that form the east and west boundaries of the Salavatlı geothermal field; the first outcrop is exposed in Yavuzköy village and the second outcrop is between Güvendik-Malgaçemir villages and Sultanhisar.

Table 2. XRD results for well AS-1 clay samples.

Sample	Well depth (m)	Temperature (T °C)	Air-dried lines dÅ	Mg-ethylene glycol lines dÅ	K-550 °C lines dÅ	K-700 °C lines dÅ	Probable minerals
7657	6	52.1	10.15 7.18	17.32 10.04 7.13	10.15		less montmorillonite illite kaolinite
7658	50	52.1	10.04 7.13	17.32 10.04 7.19	10.04		montmorillonite illite kaolinite
8231	287	64.6	10.04 7.13	10.04 7.13	10.04 7.13	10.04	illite dickite
7927	312	64.6	10.15 7.22	17.65 10.15 7.22	10.15		montmorillonite illite kaolinite
7928	328	64.6	10.22 7.22	17.65 10.15 7.22	10.15 7.22		montmorillonite illite kaolinite
7930	502	70.9	10.04 7.13	10.08 7.15	10.08		illite kaolinite
7931	556	77.1	10.04 7.13	17.51 10.15 7.18	10.15		montmorillonite illite kaolinite
7932	566	77.1	10.08 7.18	10.15 7.18	10.04		illite kaolinite
7933	576	77.1	11.04 10.04 7.15	10.04 7.13	10.04		hydrobiotite illite kaolinite
8232	576	77.1	13.18 10.64 9.92	15.23 9.82	10.04		chlorite montmorillonite illite
8233	583	77.1	13.38 10.59	14.96 13.18 9.93	10.07		vermiculite chlorite illite
7934	682	88.1	10.04 7.18	9.99 7.13	9.99		illite kaolinite
8234	682	88.1	12.61 9.98 7.10	16.99 9.93 7.13	10.04		montmorillonite illite kaolinite
7935	706	88.1	10.04	10.04	10.04		illite
8235	706	88.1	9.92 7.07	9.92 7.07	9.92		illite chlorite
7938	732	101.3	10.04	10.04	10.04		illite
8239	766	122.6	9.92	9.92	9.92		illite
8240	778	127.6	9.86 7.13	9.92 7.19	9.98		illite kaolinite
8242	990	131.9	10.04	9.98	9.98		illite
8243	1100	162.75	9.92	9.93	9.93		illite

Table 3. Analyses of spring waters and well waters (well head) from the Aydın-Salavatlı geothermal field.

Location	Malgaçemir spring	Salavatlı spring	AS-1 well	AS-2 well
Temp. °C	30	40.5	169.77	175.62
pH	7.3	6.1	8.7	7.7
K^+ (mg/l)	2.4	3.6	85	90
Na^+ "	12	45	1500	1100
Ca^{++} "	76	104	6	14
Mg^{++} "	35	204	0.0	1.1
Cl^- "	43	16	297	233
B^{+++} (total)	< 0.1	< 0.1	66	42
SO_4^{--} "	50	298	196	170
HCO_3^- "	342	1025	3208	2831
SiO_2 "	25	43	135	178
Calculated reservoir temperature (°C)			160	175

Table 4. Well AS-1 temperature measurements (T °C).

	17.07.1987	19.07.1987	19.07.1987	19.07.1987	20.07.1987	20.07.1987	20.07.1987	21.07.1987	22.07.1987	28.07.1987	16.09.1996
Depth (m)	Number 1	Number 2	Number 3	Number 4	Number 5	Number 6	Number 7	Number 8	Number 9	Number 10	Number 11
0.00		91.0	52.1			60.9	58.6			53.04	24.83
100.00										84.73	44.03
200.00										100.46	76.62
250.00	70.8	108.6	64.6	83.0	60.1	79.8	143.5	100.6	42.8		
300.00										119.28	101.72
400.00										130.22	119.97
500.00	82.0	119.9	70.9	100.0	87.5	92.0	152.0	119.5		136.68	126.11
600.00	91.5	126.3	77.1							146.41	150.86
700.00	96.3	132.9	88.1	109.9	106.4	109.8	156.5	138.2	44.6	157.34	158.75
750.00	97.8	144.2	101.3	132.6	116.0	118.0	157.4	144.2	47.3		165.70
760.00				122.6	122.7	126.1	158.3	148.6	48.8		
770.00				127.6	131.1	135.1	159.8	152.6	51.2		
780.00				137.1	143.4	145.5	162.1	160.6	52.2		
790.00				137.1	142.2	144.3	160.8	160.6	53.8		
800.00	99.9	143.5	117.4	134.9	139.4	141.9	159.7	160.2	59.0	163.90	169.46
850.00	100.1	131.7	119.7	125.7	130.4	133.7	158.7	157.5	64.2		169.77
900.00	101.9	128.4	131.7	131.9	132.4	133.1	160.6	156.0	68.9	167.00	167.58
950.00	102.2	126.2	131.0	132.6	133.8	134.0	152.6	152.4	75.4		166.80
980.00				131.9	133.2	133.9	149.9	150.6	82.5		
990.00				131.9	133.2	133.5	149.6	149.8	86.2		
1000.00	103.2	125.5	130.4	132.1	133.3	133.7	149.2	149.1	90.4	165.16	165.33
1050.00	102.8	124.9	129.9	131.1	132.4	132.8	149.1	147.3	102.7		163.56
1100.00	103.2	125.1		131.5	132.3	132.8	148.9	145.7	118.6	162.75	162.70
1150.00	103.2	125.1	129.9	131.6	132.6	132.9	149.4	145.1	132.8		160.48
1200.00	103.8	125.7	130.5	131.8	132.3	133.2	149.6	145.6	145.3	160.10	159.22
1250.00	105.5	127.3	132.0	133.3	134.4	134.5	148.9	146.0	145.6		157.92
1300.00	106.4	128.2	133.1	134.4	135.8	135.8	148.4	145.5	145.7	157.00	157.03
1350.00	106.4	128.4	132.7	134.6	135.9	135.9	148.6	145.2	145.8		156.46
1400.00	107.9	130.9	135.6	137.0	138.1	138.6	151.2	147.1	146.4	155.50	156.88
1438.65											158.18
1450.00	113.2	136.5	140.9	142.3	143.4	143.3	153.7	150.97	150.9		
1458.00										155.73	
1494.00				144.1	145.1	145.2	155.7	153.7	152.5		
1500.00	129.3	138.2	143.0								

Table 5. Well AS-2 temperature measurements (T °C).

	21.01.1988	22.01.1988	22.01.1988	25.01.1988	27.01.1988	27.01.1988	27.01.1988	27.01.1988	1.02.1988	17.09.1996
Depth (m)	Number 1	Number 2	Number 3	Number 4	Number 5	Number 6	Number 7	Number 8	Number 9	Number 10
0.00				150.9						24.08
100.00	48.3	55.2			52.5				43.3	43.51
200.00	57.9	68.6			66.7				61.2	67.35
300.00	61.4	84.5			83.2				81.0	90.22
400.00	62.2	97.2			103.1				99.1	112.27
500.00	72.1	110.2	103.1		121.2				117.4	130.70
600.00	86.6	112.9	114.7		134.4				132.2	148.13
700.00	102.8	128.2	120.7		145.7				146.8	162.10
767.00				162.6						169.98
768.00							148.6	154.0		
800.00	110.6	129.1	132.7		159.3	44.9	152.2	157.5	165.1	174.26
808.00	121.3	135.2	139.2	166.4	162.9	59.4	152.9	158.5	167.6	
825.00						59.8	154.0	159.2		
850.00	124.2	137.8	142.6	168.3	163.8	71.0	151.7	159.0	167.8	175.30
875.00						73.9	150.4	157.5		
900.00	127.0	141.8	145.7	169.1	165.3	75.9	149.2	156.0	168.3	175.62
910.00						78.4	146.5	154.7		
920.00						79.5	145.4	154.0		
921.00		146.2				80.8				
925.00			149.0							
928.00	133.1			170.2	166.1				168.6	
930.00							144.8	153.7		
934.00				170.7	166.9				168.6	175.56
935.00						81.9	138.2	150.2		
938.7				171.1						
940.00					168.6		134.0	146.4		
940.5									169.7	
940.9										
942.00						86.3				

Evidence of surface mineralization is also present in the cuttings of the AS-1 and AS-2 wells. Mineral products of hydrothermal activity (Table 1), including quartz, calcite, dolomite, siderite, pyrite, kaolinite, dickite (seen at 378 m within Miocene sandstone of AS-1 borehole, as an acidic alteration), montmorillonite, illite, (seen above the lost circulation zone as the product of scaling and cap rock in AS-1), hydrobiotite, vermiculite (seen at 583 m in AS-1), sericite, chlorite, albite, limonite, and opaque minerals, have been noted in the AS-2 and AS-1 wells.

X-ray diffraction analyses were done on selected ≅4 mm samples of cuttings to identify and confirm the types of clay minerals present in the cuttings. Especially detailed study was done on well number AS-1. Relevant data are given in Table 2.

XRD analyses for clay minerals were done on samples taken from several depths in the AS-1 and AS-2 wells, and indicate the presence of montmorillonite, illite, chlorite, vermiculite, hydrobitite and dickite. Figures 5 and 6 show two well sections with five different clay zones distinguished. From top to bottom they are as follows: a mixed-layer clay zone, an illite-kaolinite zone, a chlorite-illite zone, an illite-montmorillonite zone and a chlorite-epidote zone.

Albitization and chloritization in the metamorphic sequences of AS-1 and particularly in AS-2 were clearly observed. Miocene sediments in the same wells show acidic alteration such as dickite. Vermiculite, observed at the base of the gneisses, indicates the presence of a nearby intrusive body which apparently intruded the floor

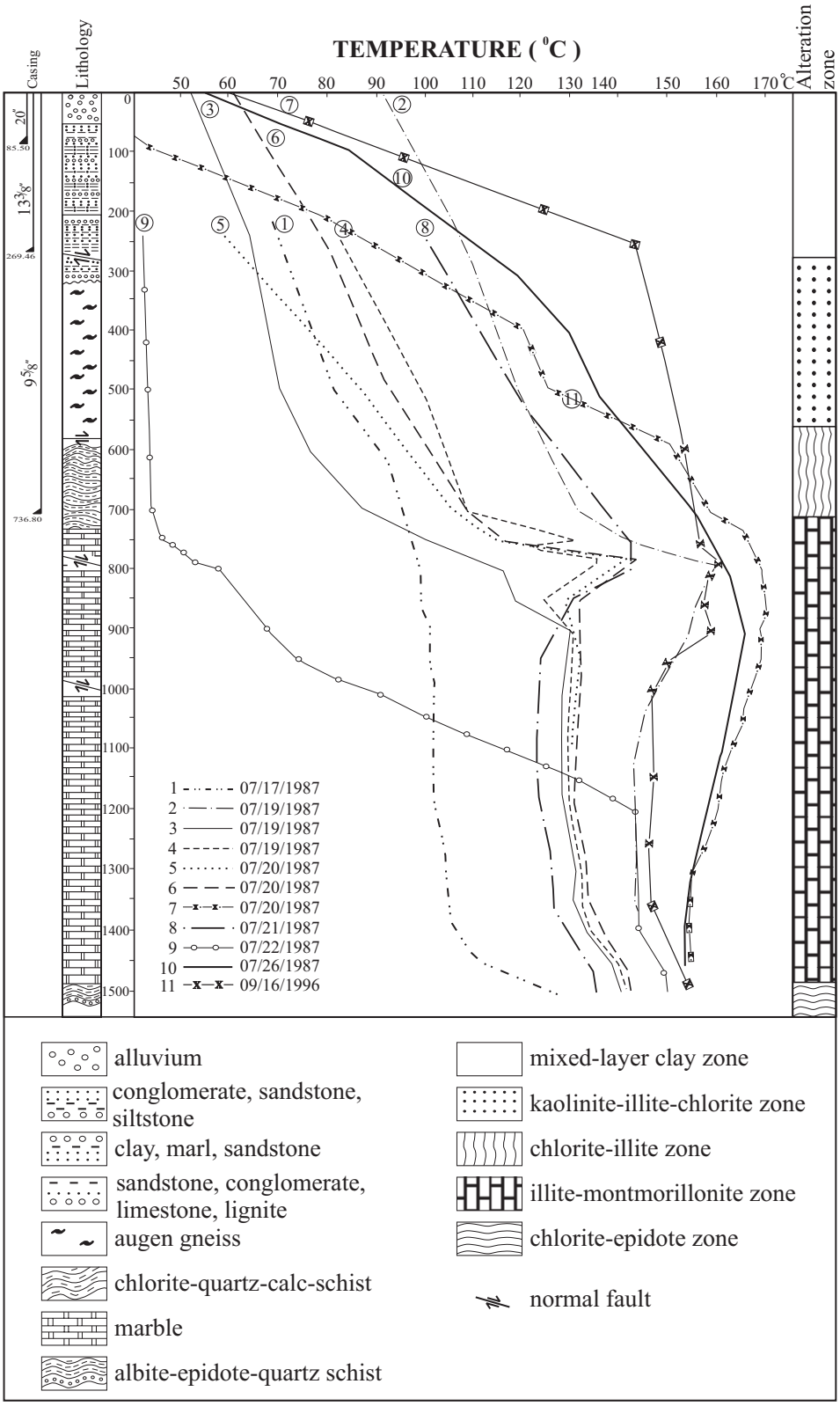

Figure 5. Well log and temperature profile of the AS-1 well (see Figure 2 for location).

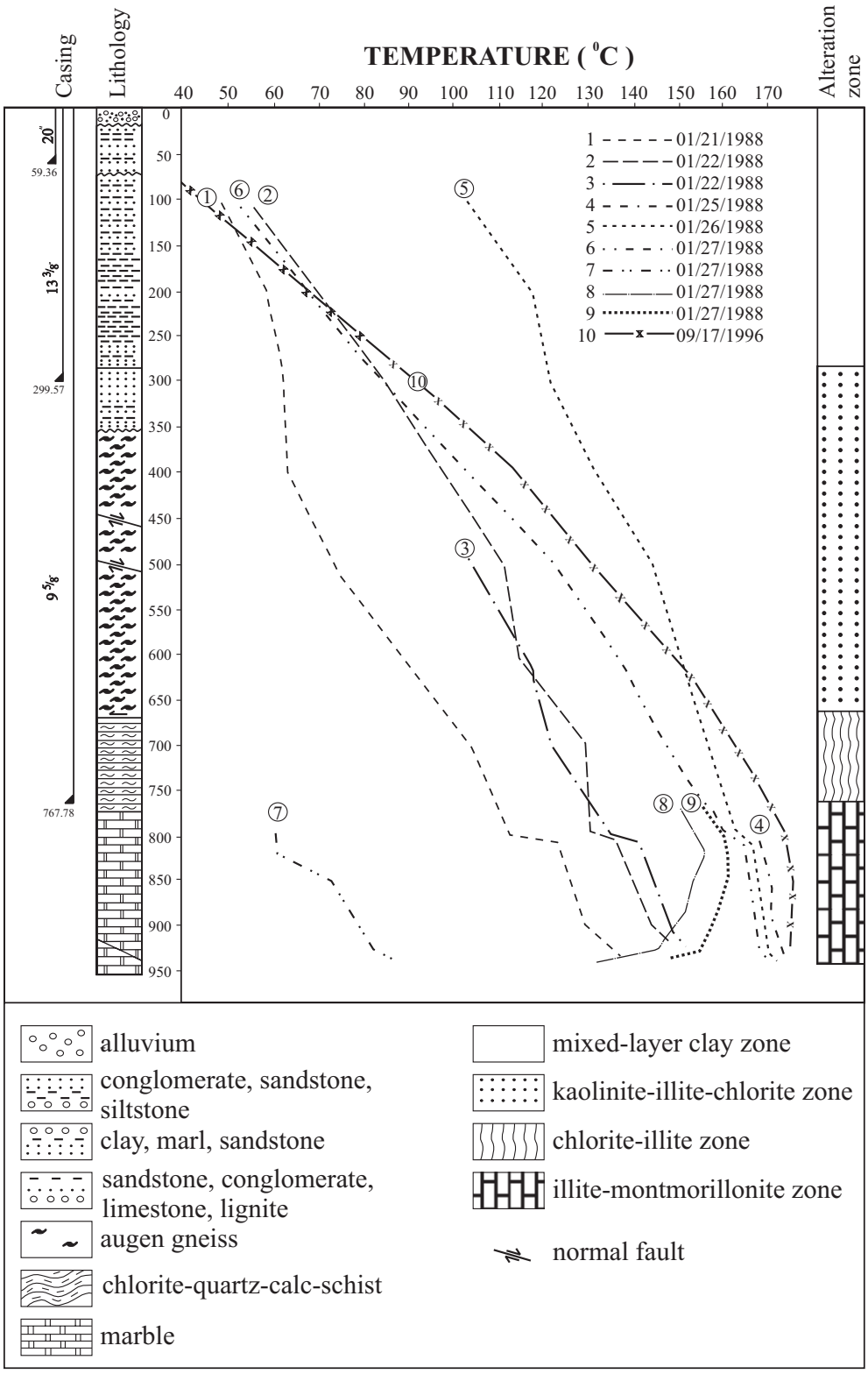

Figure 6. Well log and temperature profile of the AS-2 well (see Figure 2 for location).

of the graben (Boles 1977). Feldspar, garnet, muscovite, biotite, tourmaline, rutile, apatite, graphite, cristobalite and epidote observed in the same zones are either early high-temperature products of hydrothermal alteration or relict minerals from regional metamorphism (Table 1). Albite, chlorite, vermiculite, dickite, quartz, calcite, kaolinite, dolomite, montmorillonite, and illite are products of hydrothermal alteration and occur as vein fillings and in vesicules (Table 2). These minerals indicate a temperature range between 150°C and 300°C (Henley & Ellis 1983).

An NE–SW cross-section through the AS-1 and AS-2 wells (Figure 4) suggests that the NE–SW fault systems passing through marble are the production zone for geothermal fluids in the region. Well-finishing testing was completed for the AS-1 well. Eleven temperature measurements were taken during the well testing (Table 4). These temperature measurements indicate that the reservoir of this field is a horizontal-flow type located within the fault zones between 750–780 m and 990–1000 m. Temperature measurements are given in Figure 5. A negative thermal gradient was measured at 1000 m depth in the AS-1 well. Stefansson & Steingrimsson (1981) showed that there is a negative gradient below the horizontal-flow zone in the horizontal-flow system.

The AS-2 well was terminated at a depth of 962 m where complete loss of circulation was attained. Well-finishing testing was completed for the AS-2 well. Ten temperature measurements were taken during the well testing (Table 5). These temperature measurements indicate that the reservoir of this cross-fault zone is located between 750 and 950 m. The temperature measurements are given in Figure 6. Total discharge data are as follows: WHP (bar.g) 2; Pc (psig) 11; total production is calculated at 313.2 t/h. WHP (bar.g) is 14.5. The maximum temperatures measured in the AS-1 and AS-2 wells were 169.77ºC and 175.62ºC, respectively. These maximum temperatures were recorded between 770 and 990 m in both wells. Below this level, the temperature in AS-1 decreased to 155ºC. These temperature data indicate that the fault systems control the geothermal activity in the area, and that the maximum attainable reservoir temperature can be found to the south where the normal-fault systems are both younger and deeper (see Figure 3).

Geophysical Survey

Gravity surveys were used to outline regional tectonic structures such as the main fault systems along horst and graben boundaries. Positive anomalies on the second-order derivative gravity map suggest that there are hidden horsts within the graben in the vicinity of Salavatlı, Sultanhisar and Köşk (Gülay 1988) (Figure 7).

Resistivity surveys were completed to delineate the geothermal reservoir system by means of its low resistivity values (Griffiths & King 1969). An apparent resistivity map was plotted with a half electrode distance of 700 m, which reflects the resistivity features at a depth of 700 m (Figure 8). It should be noted that there are two distinct resistivity anomaly trends extending from NE to SW and from NW to SE. These represent the normal-faulted boundaries of the horst and graben structures between Salavatlı and Köşk. The resistivity map frames a roughly triangular area characterized by very low resistivity contours (5–10 ohm). Such areas, with resistivity values much lower than the background resistivity, are generally classified as high-potential, geothermal energy target areas in the Büyük Menderes Graben (Şahin 1985).

Geoelectric and Bouguer gravity anomaly cross-sections along traverse lines D-1680 and D-2040 (Figures 9 & 10) suggest a structural relationship between the metamorphic basement and the Neogene cover. The lowest resistivity in this area is located on the northern flank of the graben above the step-faulted basement. These lower resistivities apparently result from the circulation of super-heated geothermal fluid along the heavily fractured active fault zones in the basement. Deep exploratory drilling to intersect these supposed active fault zones at deeper levels is suggested for the future assessment of the Aydın-Salavatlı geothermal field. It is obvious that more deep drilling is necessary in order to explain the detailed characteristics of this field.

Discussion and Conclusion

The thermal systems of western Turkey exhibit a wide range of chemical compositions that reflect the complex nature and different sources of thermal waters. Vengosh *et al.* (2002) distinguish four major groups that reflect different origins and mechanisms of water-rock interactions.

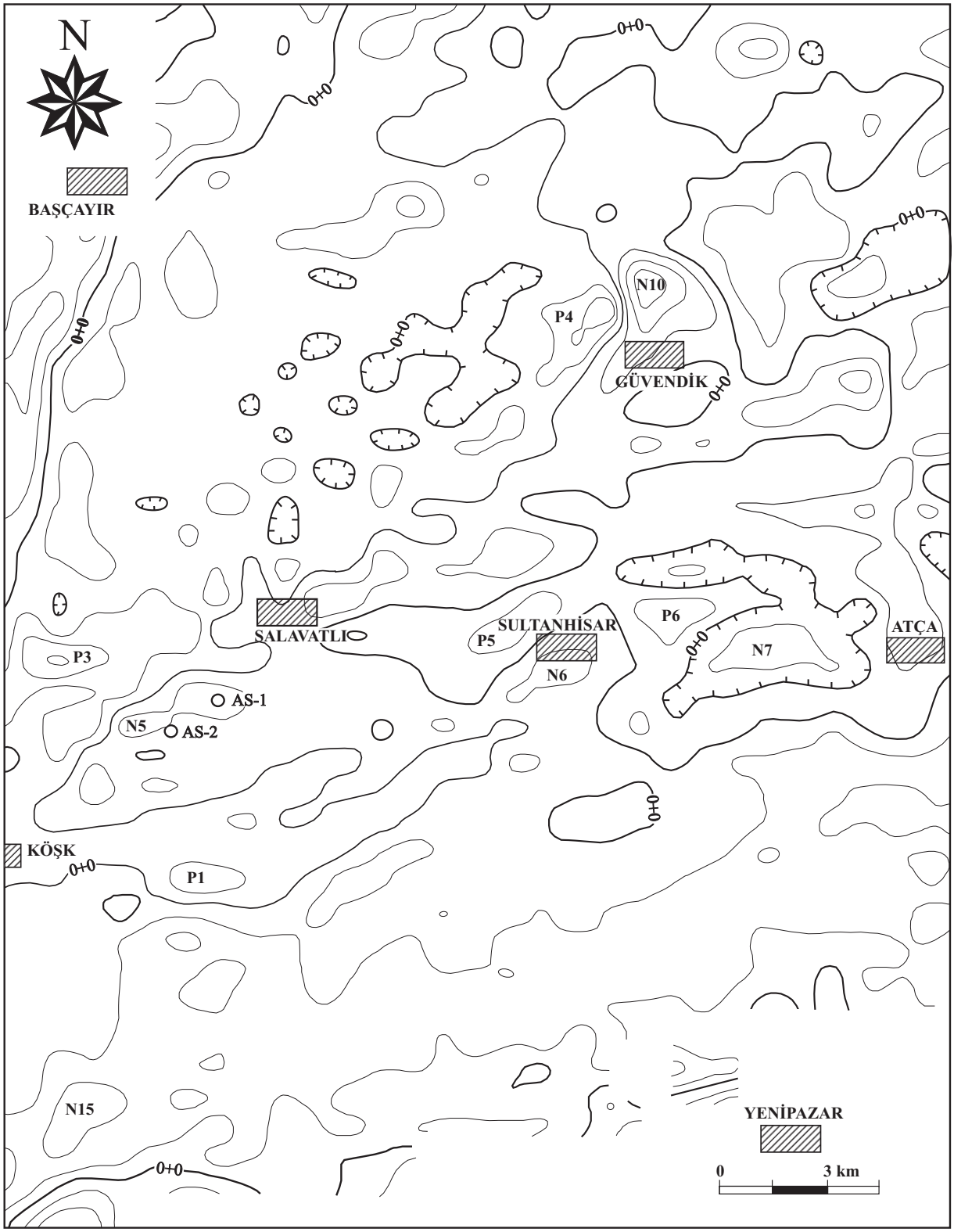

Figure 7. Second-order gravity map of the Aydın-Salavatlı geothermal field (after Gülay 1988).

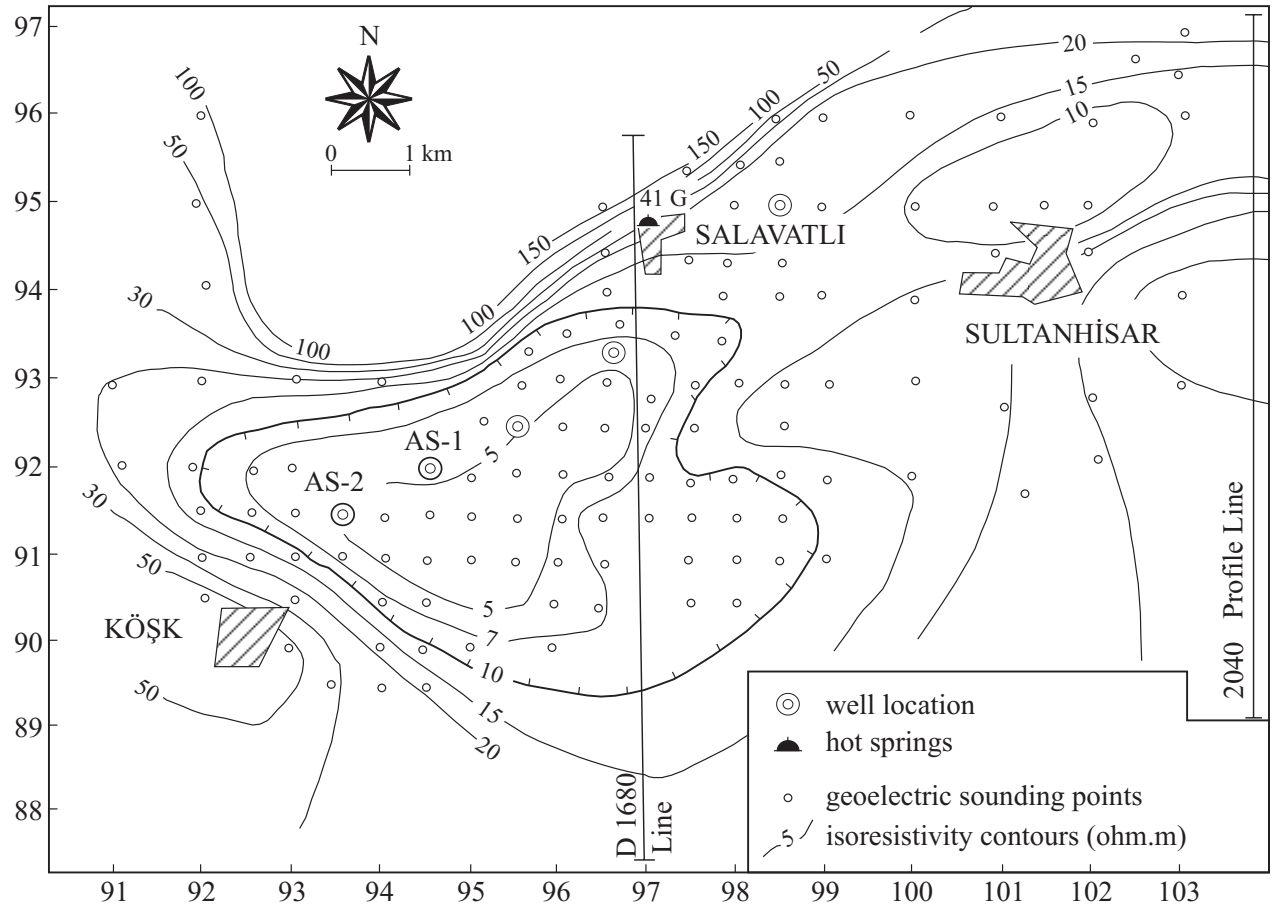

Figure 8. Apparent resistivity map of the Aydın-Salavatlı geothermal field (after Şahin 1985).

Vengosh *et al.* (2002) showed that the chemical data, combined with isotopic data for boron and strontium of thermal waters from western Turkey, reveal four types of water, which originated from marine and non-marine sources. The marine source has a Na-Cl composition and Na/Cl ratio<1 whereas the non-marine water typically has Na/Cl>1. The Br/Cl ratio is used to distinguish between direct penetration of seawater or recycled marine salts in the form of evaporite dissolution. The non-marine water shows three types of chemical compositions, reflecting different source rocks and depth of circulation. Na-HCO_3 and Na-SO_4 compositions reflect deep circulation and interactions with metamorphic rocks while Ca-Mg-SO_4-HCO_3 composition is associated with shallow circulation in carbonate rocks and mixing with cold ground water. The $^{87}Sr/^{86}Sr$ ratio further constrains the nature of the source rocks (i.e. igneous and metamorphic versus carbonate rocks). Systematic changes in sodium, potassium, calcium, and magnesium with temperature show that concentrations of these dissolved constituents are largely dependent on the temperature and depth of circulation. Water-rock interaction results in high concentrations of dissolved constituents such as Na, K, and B. The data suggest that boron is derived from water-rock interaction rather then deep mantle flux of $B(OH)_3$ gas. The high boron concentration in the thermal water is typical of many non-marine geothermal fields, worldwide, and thus can be used as a sensitive tracer to monitor advection and mixing of underlying geothermal fluids with shallow groundwater (Vengosh *et al.* 2002).

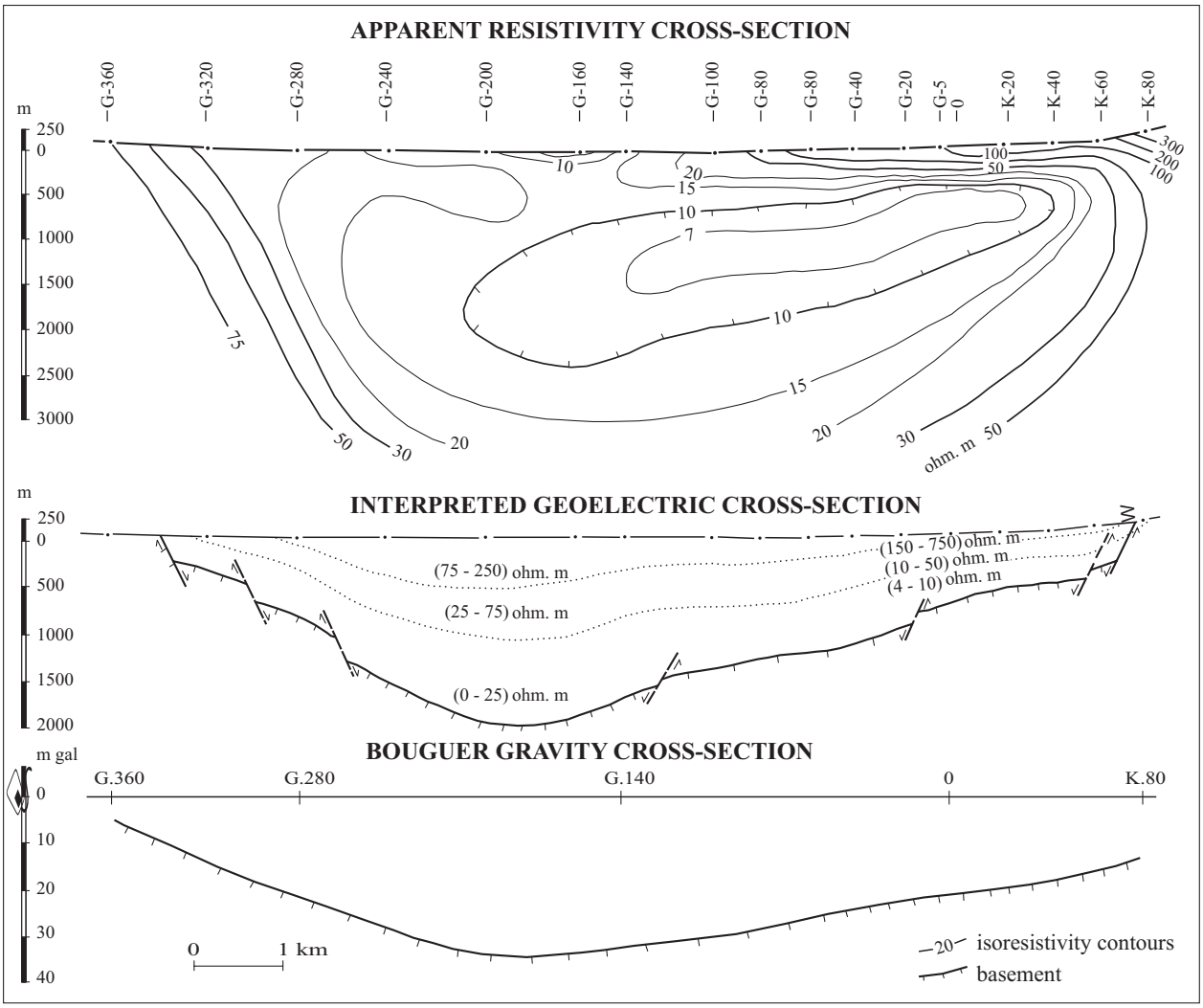

Figure 9. N–S cross-sections of resistivity, geoelectric and Bouguer gravity along traverse line-1680, town of Salavatlı (after Şahin 1985).

Thermal waters from western Turkey have typically high boron contents which present environmental and operational problems. The association of high boron and high CO_2 levels led Tarcan (1995) to suggest that the boron was derived from a deep mantle source. Also, Demirel and Şentürk (1996) suggested that high B, NH_4, and CO_2 concentrations in thermal water from the Kızıldere geothermal field reflect ascent of magmatic emanation from depth although there is no evidence of recent volcanic activity in the area. Based on $^3He/^4He$ ratios, Güleç (1988) argued that the involvement of mantle-derived helium in Kızıldere geothermal field does not exceed 30%.

Two models should therefore be considered for the origin of boron in the thermal water: (1) dissolved Cl, HCO_3, and B are derived from deep mantle flux of HCl, CO_2 and $B(OH)_3$ gases; or (2), water-rock interactions leach boron to the liquid phase (Vengosh *et al.* 2002).

Karamanderesi & Helvacı (1994) and Karamanderesi (1997) measured REE and other elements extracted from well cuttings and core samples from different geothermal fields and surface rock samples in the Menderes Massif. Their data showed that:

1. Different rock units from the Salavatlı geothermal field have high concentrations of boron (range of 800 to 1600 ppm) relative to those (independent

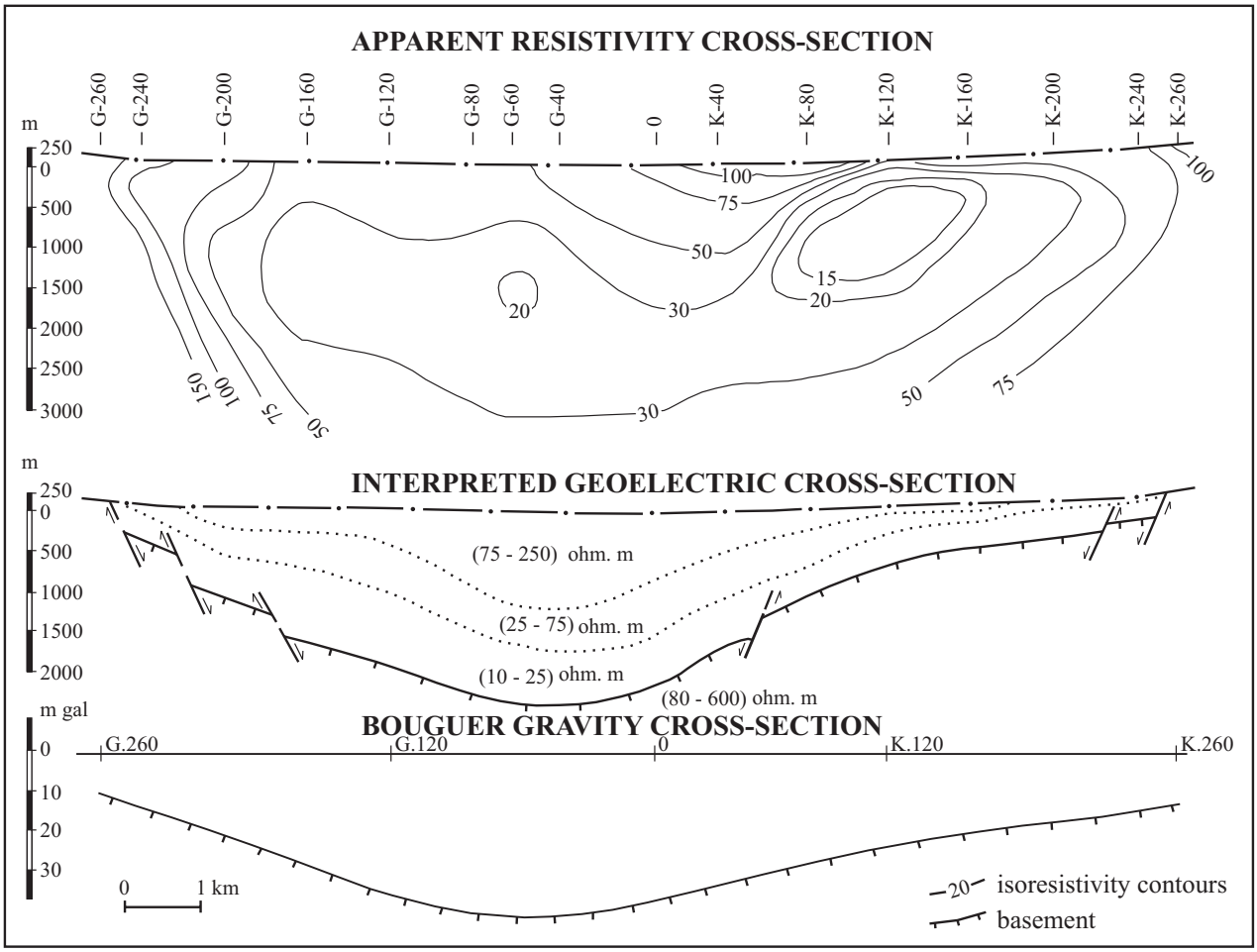

Figure 10. N–S cross-sections of resistivity, geoelectric and Bouguer gravity along traverse line D-2040, east of Sultanhisar (after Şahin 1985).

on lithology) of the Ömerbeyli field (a range of 50–230 ppm). The difference in the boron contents of the rocks is also reflected in the relatively higher B/Cl ratio in the associated thermal waters from these two systems (0.7 relative to 0.1), whereas the absolute boron concentrations are similar.

2. Boron is unevenly distributed among different rock types. Boron is particularly enriched in (decreasing order) quartz veins, tourmaline gneiss, the illite-chlorite-feldspar zone, and the quartz-chlorite schist zone. Boron is relatively depleted in marble and gabbro.

3. The vertical distribution of boron (and lithium) with depth is not uniform and is heavily dependent on lithology. Boron is depleted in the marble zone of the Ömerbeyli field (~50 ppm B at depth of 1400 m) relative to the albite-amphibolite schist zone (~200 ppm, ~1400 m).

If indeed all of the boron was derived from deep mantle flux as argued by Tarcan (1995) one would expect to have uniform boron composition with similar B/Cl ratios in all of the thermal systems. Moreover, one would not expect to have any relationships between B contents in local rocks and thermal waters. And yet, the Salavatlı geothermal field is significantly enriched in boron relative to the Ömerbeyli field (Vengosh *et al.* 2002). Consequently, it seems that boron is mainly derived from local water-rock interactions and the source rocks strongly control the boron levels of the water (e.g.,

quartz vein or tourmaline gneiss versus marble). Nevertheless, the overall boron budget of a geothermal system can also be controlled by the original boron concentrations in the rock or original parent magma fluids, as well as by the degree of maturation in which water-rock interactions can contribute boron to the thermal system.

In this study, an attempt has been made to clarify the relative timing of the neotectonic and palaeotectonic episodes. Gabbroic and acidic dykes developed and were emplaced during the neotectonic period. The approximate locations of the heat source and alteration zones have been outlined within the study area.

The following alteration minerals are attributed to geothermal activity in the area: quartz, albite, chlorite, calcite, aragonite, dolomite, kaolinite, illite, montmorillonite, specular haematite, gypsum, dickite, vermiculite, pyrite, siderite and hydrobiotite.

The mineral paragenesis of chlorite, calcite, illite, kaolinite, dickite, montmorillonite, pyrite, and hydrobiotite in the area indicates a reservoir temperature of approximately 200ºC, which is considerably higher than the temperatures predicted by geothermometers for AS-1 (169.77ºC) and AS-2 (175.62ºC) wells. Geological and geophysical studies indicate that geothermal activity in the area is closely related to active fault systems. The fault systems and surrounding related fractures bound the geothermal reservoir.

A new drilling site is suggested for future production drilling, in the southern part of the area where tectonic activity is younger and deeper, and from which higher reservoir temperatures may likely be obtained.

Acknowledgements

Fieldwork was supported by the General Directorate of Mineral Research and Exploration (MTA) (Ankara) and the MTA İzmir Branch Office. We thank the management and technical staff of MTA for their assistance. We would like to thank Steven K. Mittwede and Hasan Sözbilir for critically reading the manuscript, and İbrahim Arpalıyiğit for his assistance with writing and drafting. We appreciate and thank the anonymous reviewers for their thorough review of an earlier version of the manuscript. This study was also supported by a research project grant (Project Number AIF–0922.93.05.04) from Dokuz Eylül University, Graduate School of Natural and Applied Sciences.

References

AKARTUNA, M. 1965. Aydın-Nazilli hattı kuzeyindeki versanların jeolojisi hakkında [About the geology of Aydın-Nazilli region]. *General Directorate of Mineral Research and Exploration (MTA) Bulletin* **65**, 1–10 [in Turkish with English abstract].

BOLES, J.R. 1977. Zeolite in low-grade metamorphic grades. Mineralogy and geology of natural zeolites. *In*: MUMPTON, F.A. (ed), *Mineralogical Society of America Short Course Notes* **4**, 103–135.

BOZKURT, E. 1995. Deformation during main Menderes metamorphism (MMM) and its tectonic significance: evidence from southern Menderes Massif, western Turkey. *Terra Abstracts* **7**, p. 176.

BOZKURT, E. 2000. Timing of extension on the Büyük Menderes Graben, western Turkey and its tectonic implications. *In:* BOZKURT, E., WINCHESTER J.A. & PIPER, J.D.A. (eds), Tectonics and Magmatism in Turkey and the Surrounding Area. *Geological Society, London, Special Publications* **173**, 385–403.

BOZKURT, E. 2001a. Neotectonics of Turkey – a synthesis. *Geodinamica Acta* **14**, 3–30.

BOZKURT, E. 2001b. Late Alpine evolution of the central Menderes Massif, western Anatolia, Turkey. *International Journal of Earth Sciences* **89**, 728–744.

BOZKURT, E. 2002. Discussion on the extensional folding in the Alaşehir (Gediz) Graben, western Turkey. *Journal of the Geological Society, London* **159**, 105–109.

BOZKURT, E. & OBERHÄNSLI, R. 2001a. Menderes Massif (western Turkey): structural, metamorphic and magmatic evolution – a synthesis. *International Journal of Earth Sciences* **89**, 679–708.

BOZKURT, E. & OBERHÄNSLI, R. (eds) 2001b. Menderes Massif (western Turkey): structural, metamorphic and magmatic evolution. *International Journal of Earth Sciences Special Issue* **89**, 679–882.

BOZKURT, E. & PARK, R.G. 1994. Southern Menderes Massif: an incipient metamorphic core complex in western Anatolia, Turkey. *Journal of Geological Society, London* **151**, 213–216.

BOZKURT, E. & PARK, R.G. 1997a. Evolution of a mid-Tertiary extensional shear zone in the southern Menderes Massif, Western Turkey. *Societe Geologique de France Bulletin* **168**, 3–14.

BOZKURT, E. & PARK, R.G. 1997b. Microstructures of deformed grains in the augen gneisses of the southern Menderes Massif and their tectonic significance. *Geologische Rundschau* **86**, 103–119.

BOZKURT, E. & PARK, R.G. 1999. The structure of the Palaeozoic schists in the southern Menderes Massif, western Turkey: a new approach to the origin of the main Menderes metamorphism and its relation to the Lycian Nappes. *Geodinamica Acta* **12**, 25–42.

BOZKURT, E. & SATIR, M. 2000. New Rb-Sr geochronology from the southern Menderes Massif (southwestern Turkey) and its tectonic significance. *Geological Journal* **35**, 285–296.

BOZKURT, E., PARK, R.G. & WINCHESTER, J.A. 1993. Evidence against the core/cover interpretation of the southern sector of the Menderes Massif, west Turkey. *Terra Nova* **5**, 445–451.

BOZKURT, E., WINCHESTER, J.A. & PARK, R.G. 1995. Geochemistry and tectonic significance of augen gneisses from the southern Menderes Massif (West Turkey). *Geological Magazine* **132**, 287–301.

ÇAĞLAR, K.Ö. 1961. Türkiye maden suları ve kaplıcaları [Mineral waters and thermal springs of Turkey]. *General Directorate of Mineral Research and Exploration (MTA) Bulletin* **107**, I–4, Ankara [in Turkish with English abstract].

ÇAĞLAYAN, M.A., ÖZTÜRK, E.M., ÖZTÜRK, Z., SAV, H. & AKAT, U. 1980. Menderes Masifi güneyine ait bulgular ve yapısal yorum [Evidence from the southern Menderes Massif and structural interpretation]. *Jeoloji Mühendisliği* **10**, 9–19 [in Turkish with English abstract].

CANDAN, O. 1995. Menderes Masifinde kalıntı granulit fasiyesi metamorfizması [Relict granulite facies metamorphism in the Menderes Massif]. *Turkish Journal of Earth Sciences* **4**, 35–55 [in Turkish with English abstract].

CANDAN, O. 1996. Çine Asmasifindeki (Menderes Masifi) gabroların metamorfizması ve diğer asmasiflerle karşılaştırılması [Metamorphism of gabbros in the Çine submassif (Menderes Massif) and comparison with other submassifs]. *Turkish Journal of Earth Sciences* **5**, 123–139 [in Turkish with English abstract].

CANDAN, O. & DORA, O.Ö. 1998. Granulite, eclogite and bluschist relics in the Menderes Massif: an approach to Pan-African and Tertiary metamorphic evolution. *Geological Society of Turkey Bulletin* **41**, 1–35 [in Turkish with English abstract].

CANDAN, O., DORA, O.Ö., OBERHÄNSLI, R.,OELSNER, F.C. & DÜRR, S. 1997. Blueschist relics in the Mesozoic series of the Menderes Massif and correlation with Samos island. *Schweizerische Mineralogische und Petrographische Mitteilungen* **77**, 95–99.

CANDAN, O., DORA O.Ö., OBERHÄNSLI, R., ÇETİNKAPLAN, M., PARTZSCH, J.H., WARKUS, F.C. & DÜRR, S. 2001. Pan-African high-pressure metamorphism in the Precambrian basement of the Menderes Massif, western Anatolia, Turkey. *International Journal of Earth Sciences* **89**, 793–811.

COLLINS, A.S. & ROBERTSON, A.H.F. 1997. Processes of Late Cretaceous to Late Miocene episodic thrust-sheet translation in the Lycian Taurides, SW Turkey. *Journal of the Geological Society, London* **155**, 759–772.

COLLINS, A.S. & ROBERTSON, A.H.F. 1999. Evolution of the Lycian allochthon, western Turkey, as a north-facing Late Palaeozoic rift and passive continental margin. *Geological Journal* **34**, 107–138.

DEMİREL, Z. & ŞENTÜRK, N. 1996. Geology and hydrogeology of deep thermal aquifers in Turkey. *In*: AL-BEIRUTI, S.N. & BINO, M.J. (eds), *Integration of Information Between Oil Drilling and Hydrogeology of Deep Aquifers.* The Inter-Islamic Network of Water Resources Development and Management, Royal Scientific Society Printing Press, Amman, Jordan, 387–403.

DEWEY, J.F. 1988 Extensional collapse of orogens: *Tectonics* **7**, 1123–1139.

DEWEY, J.F. & ŞENGÖR, A.M.C. 1979 Aegean and surrounding regions: complex multiplate and continium tectonics in a convergent zone. *Geological Society of America Bulletin* **90**, 84–92.

DORA, O.Ö., KUN, N. & CANDAN, O. 1992. Metamorphic history and geotectonic evolution of the Menderes Massif. *In*: SAVAŞÇIN, M.Y. & ERONAT, A.H. (eds), *IESCA–1990 Proceedings, International Earth Science Congress on Aegean Regions*, İzmir, 102–115.

DÜRR, S., ALTHERR, R., KELLER, J., OKRUSCH, M. & SEIDEL, E. 1978. The median Aegean crystalline belt: stratigraphy, structure, metamorphism and magmatism. *In*: CLOSS, H., ROEDER, D.R. & SCHMIDT, K. (eds) *Alps, Apennines, Hellenides*, 455–477. Schweizerbart, Stuttgart.

ERCAN, T., SATIR, M., KREUZER, H., TÜRKECAN, A., GÜNAY, E., ÇEVİKBAŞ, A., ATEŞ, M. & CAN, B. 1985. Batı Anadolu Senozoyik volkanitlerine ait yeni kimyasal, izotopik, ve radyometrik verilerin yorumu [Interpretation of new geochemical, isotopic and radiometric data from Cenozoic volcanics of west Turkey]. *Geological Society of Turkey Bulletin* **28**, 121–136 [in Turkish with English abstract].

EYİDOĞAN, H. 1988. Rates of crustal deformation in western Turkey as deduced from major earthquakes. *Tectonophysics* **148**, 83–92.

GENÇ, Ş.C., ALTUNKAYNAK, Ş., KARACIK, Z. YAZMAN, M. & YILMAZ, Y. 2001. The Çubukdağ graben, south of İzmir: its tectonic significance in the Neogene geological evolution of the western Anatolia. *Geodinamica Acta* **14**, 45–56.

GESSNER, K., PIAZOLO, S., GÜNGÖR, T., RING, U., KRÖNER, A. & PASSCHIER, C.W. 2001a. Tectonic significance of deformation patterns in granitoid rocks of the Menderes nappes, Anatolide belt, southwest Turkey. *International Journal of Earth Sciences* **89**, 766–780.

GESSNER, K., RING, U., CHRISTOPHER, J., HETZEL, R., PASSCHIER, C.W. & GÜNGÖR, T. 2001b. An active bivergent rolling-hinge detachment system: Central Menderes metamorphic core complex in western Turkey. *Geology* **29**, 611–614.

GIGGENBACH, W.F. 1986. Graphical techniques for the evaluation of water/rock equlibration conditions by use of Na, K, Mg and Ca-contents of discharge waters. *Proceedings of the 8th Geothecnical Workshop*, Auckland, New Zealand, 37–44.

GÖKTEN, E., HAVZAOĞULU, Ş. & ŞAN, Ö. 2001. Tertiary evolution of the central Menderes Massif based on structural investigations of metamorphics and sedimentary cover rocks between Salihli and Kiraz (western Turkey). *International Journal of Earth Sciences* **89**, 745–756.

GRACIANSKY, P.C. 1972. *Reserches gèologiques dans le Taurus Lycien occidental.* Thèse, University de Paris-Sud, Orsay.

GRIFFITHS, D.H. & KING, R.F. 1969. *Applied Geophysics*. Pergamon Press, Great Britain.

GÜNGÖR, T. & ERDOĞAN, B. 2002. Tectonic significance of mafic volcanic rocks in a Mesozoic sequence of the Menderes Massif, West Turkey. *International Journal of Earth Sciences* **91**, 386–397.

GÜLAY, O. 1988. *Aydın-Nazilli Yöresi Jeofizik Gravite Etüdleri [Geophysical Investigation (Gravity Measurements) of Aydın-Nazilli Region].* General Directorate of Mineral Research and Exploration (MTA) Report No. **8322** [in Turkish, unpublished].

GÜLEÇ, N. 1988. The distribution of helium-3 in Western Turkey. *General Directorate of Mineral Research and Exploration (MTA) Bulletin* **108**, 35–42.

GÜRER, F.Ö., BOZCU, M., YILMAZ, K. & YILMAZ, Y. 2001. Neogene basin development around Söke-Kuşadası (western Anatolia) and its bearing on tectonic development of the Aegean region. *Geodinamica Acta* **14**, 57–70.

HENLEY, R.W. & ELLIS, A.J. 1983. Geothermal systems, ancient and modern: a geochemical review. *Earth Science Reviews* **19**, 1–50.

HETZEL, R. & REISCHMANN, T. 1996. Intrusion age of Pan-African augen gneisses in the southern Menderes Massif and the age of cooling after Alpine ductile extensional deformation. *Geological Magazine* **133**, 565–572.

HETZEL, R., PASSCHIER, C.W., RING, U. & DORA, O.O. 1995a. Bivergent extension in orogenic belts: The Menderes Massif (southwestern Turkey). *Geology* **23**, 455–458.

HETZEL, R., RING, U., AKAL, C. & TROESCH, M. 1995b. Miocene NNE-directed extensional unroofing in the Menderes Massif, southwestern Turkey. *Journal of Geological Society, London* **152**, 639–654.

HETZEL, R., ROMER, R.L., CANDAN, O. & PASSCHIER, C.W. 1998. Geology of the Bozdağ area, central Menderes Massif, SW Turkey: Pan-African basement and Alpine deformation. *Geologische Rundschau* **87**, 394–406.

IŞIK, V. & TEKELİ, O. 2001. Late orogenic crustal extension in the northern Menderes Massif (western Turkey): evidence for metamorphic core complex formation. *International Journal of Earth Sciences* **89**, 757–765.

JACKSON, J. & MCKENZIE, D. 1988. The relationship between plate motions and seismic moment tensors, and the rate of active deformation in the Mediterranean and Middle East. *Geophysical Journal* **93**, 45–73.

KARAMANDERESİ, İ.H. 1972. Aydın-Nazilli Çubukdağ Arası Bölgenin Jeolojisi ve Jeotermal Enerji Potansiyeli [Geology of the Aydın-Nazilli-Çubukdağ Area and Geothermal Energy Potential]. General Directorate of Mineral Research and Exploration (MTA) Report No. **5224** [in Turkish, unpublished].

KARAMANDERESİ, İ. H. 1997. *Geology of and Hydrothermal Alteration Processes of the Salavatlı-Aydın Geothermal Field.* PhD Thesis, Dokuz Eylül Üniversity Graduate School of Natural and Applied Sciences, İzmir, Turkey [unpublished].

KARAMANDERESİ, İ. H. & HELVACI, C. 1994, Geology and hydrothermal alteration of the Aydın-Salavatlı geothermal field, Western Anatolia, Turkey. *IAVCEI, 1994 Ankara, Abstract, Theme-9 Experimental Petrology.*

KARAMANDERESİ, İ.H., GÜNER, A. & ÇİÇEKLİ, K. 1987. *Aydın-Germencik-Ömerbeyli Jeotermal Sahası ÖB-8 Derin Arama Kuyusu Bitirme Raporu [Final Report on the ÖB-8 Deep-Well of Aydın-Germencik-Ömerbeyli Geothermal Field].* General Directorate of Mineral Research and Exploration Institute of Turkey (MTA) Report No. **8688** [in Turkish, unpublished].

KOÇYİĞİT, A., YUSUFOĞLU, H. & BOZKURT, E. 1999. Evidence from the Gediz graben for episodic two-stage extension in Western Turkey. *Journal of the Geological Society, London* **156**, 605–616.

KONAK, N., AKDENİZ, N. & ÖZTÜRK, E.M. 1987. Geology of the south of Menderes Massif. *Correlation of Variscan and pre-Variscan Events of the Alpine Mediterranean Mountain belt (Guide Book for the Field Excursion Along Western Anatolia, Turkey) IGCP Project No.* **5**, 42–53.

LE PICHON, X. & ANGELIER, J. 1979. The Hellenic arc and trench system: a key to the neotectonic evolution of the eastern Mediterrenean area. *Tectonophysics* **60**, 1–42.

LE PICHON, X. & ANGELIER, J. 1981. The Aegean sea. *Philosophical Transaction of Royal Society, London, Serie A* **300**, 357–372.

LIPS, A.L.W., CASSARD, D., SÖZBİLİR, H. & YILMAZ, H. 2001. Multistage exhumation of the Menderes Massif, western Anatolia (Turkey). *International Journal of Earth Sciences* **89**, 781–792.

LOOS, S. & REISCHMANN, T. 1999. The evolution of the southern Menderes Massif in SW Turkey as revealed by zircon datings. *Journal of the Geological Society, London* **156**, 1021–1030.

MCKENZIE, D.P. 1972. Active tectonics of the Mediterranean Region. *Geophysical Journal of Royal Astronomical Society* **30**, 109 p.

MCKENZIE, D.P. 1978. Active tectonics of the Alpine-Himalayan belt; The Aegean Sea and surrounding regions. *Geophysical Journal of Royal Astronomical Society* **55**, 217–254.

MEULENKAMP, J.E., WORTEL, M.J.R., VAN WAMEL, W.A., SPAKMAN, W. & HOODGERDUYN STRATING, E. 1988. On the Hellenic subduction zone and the geodynamic evolution of Crete since the late middle Miocene. *Tectonophysics* **146**, 203–215.

OBERHÄNSLI, R., CANDAN, O., DORA, O.O. & DÜRR, S. 1997. Eclogites within the Menderes Massif, western Turkey. *Lithos* **41**, 135–150.

OBERHÄNSLI, R., MONIE, P., CANDAN, O., WARKUS, F.C., PARTZSCH, J.H. & DORA, O.Ö. 1998. The age of blueschist metamorphism in the Mesozoic cover series of the Menderes Massif. *Schweizerische Mineralogische und Petrographische Mitteilungen* **78**, 309–316.

OBERHÄNSLI, R., PARTZSCH, J., CANDAN, O. & ÇETİNKAPLAN, M. 2001. First occurrence of Fe-Mg-caroholite documenting high-pressure metamorphism in metasediments of the Lycian Nappes, SW Turkey. *International Journal of Earth Sciences* **89**, 867–873.

OKAY, A.İ. 2001. Stratigraphic and metamorphic inversions in the central Menderes Massif: a new structural model. *International Journal of Earth Sciences* **89**, 709–727.

OKAY, A.İ. 2002. Reply: Stratigraphic and metamorphic inversions in the central Menderes Massif: a new structural model. *International Journal of Earth Sciences* **91**, 173–178.

OKAY, A.İ. & SIYAKO, M. 1993. The new position of the İzmir-Ankara Neo-Tethyan suture between İzmir and Balıkesir. *In*: TURGUT, S. (ed) *Tectonics and Hydrocarbon Potential of Anatolia and Surrounding Regions.* Proceedings of Ozan Sungurlu Symposium, 333–355.

OKAY, A.İ., SATIR, M., MALUSKI, H., SIYAKO, M., MONIE, P., METZGER, R. & AKYÜZ, S. 1996a. Palaeo- and Neo-Tethyan events in northwest Turkey: geological and geochronological constraints. *In*: YIN, A. & HARRISON, M. (eds), *Tectonics of Asia*. Cambridge University Press, Cambridge, 420–441.

OKAY, A.İ., TEKELİ, O., AKKÖK, R. & BOZKURT, E. 1996a. Pre-Neogene geology and tectonics of the Aegean region. *TÜBİTAK Universities-MTA National Marine Geological and Geophysical Programme, Workshop-1*, p.1–4.

ÖNAY, T.S. 1949. Über die Smirgelgesteine SW-Anatoliens. *Schweizerische Mineralogische und Petrographische Mitteilungen* **29**, 359–484.

ÖZER, S., SÖZBİLİR, H., ÖZKAR, İ., TOKER, V. & SARI, B. 2001. Stratigraphy of Upper Cretaceous-Palaeogene sequences in the southern and eastern Menderes Massif (western Turkey). *International Journal of Earth Sciences* **89**, 852–866.

PHILLIPSON, A. 1918. Kleinasien. *In*: STEINMANN, G. & WILCKENS, O. (eds), *Handbuch der Regionalen Geologie* **5**, 1–183.

RING, U., GESSNER, K., GÜNGÖR, T. & PASSCHIER, C.W. 1999. The Menderes Massif of western Turkey and the Cycladic Massif in the Aegean – do they really correlate? *Journal of Geological Society, London* **156**, 3–6.

ŞAHİN, H. 1985. *Aydın-Sultanhisar-Salavatlı Sahası Jeotermal Enerji Aramaları: Rezistivite Etüdü [Exploration for Geothermal Energy in Aydın-Sultanhisar-Salavatlı Field: Resistivity Study].* General Directorate of Mineral Research and Exploration (MTA) Report No. **7921** [in Turkish, unpublished].

SARICA, N. 2000. The Plio-Pleistocene age of Büyük Menderes and Gediz grabens and their tectonic significance on N-S extensional tectonics in West Anatolia: mammalian evidence from the continental deposits. *Geological Journal* **35**, 1–24.

SATIR, M. & FRIEDRICHSEN, H. 1986. The origin and evolution of the Menderes Massif, W-Turkey: a rubidium/strontium and oxygen isotope study. *Geologische Rundschau* **75**, 703–714.

ŞENGÖR, A.M.C. 1979. The North Anatolian transform fault: its age, offset and tectonic significance. *Journal of the Geological Society, London* **136**, 269–282.

ŞENGÖR, A.M.C. 1980. *Türkiye'nin Neotektoniğinin Esasları (Fundamentals of the Neotectonics of Turkey).* Publication of Geological Society of Turkey [in Turkish with English Abstract].

ŞENGÖR, A.M.C. 1982. Ege'nin neotektonik evrimini yöneten etkenler [Factors controlling the neotectonic evolution of Aegean]. *In*: EROL, O. & OYGÜR, V. (eds), *Batı Anadolunun Genç Tektoniği ve Volkanizması Paneli.* Geological Congress of Turkey [in Turkish with English abstract].

ŞENGÖR, A.M.C. 1987. Cross-faults and differential stretching of hanging walls in regions of low-angle normal faulting: examples from western Turkey. *In*: COWARD, M.P., DEWEY, J.F. & HANCOCK, P.L. (eds), Continental Extensional Tectonics. *Geological Society, London, Special Publications* **28**, 575–589.

ŞENGÖR, A.M.C. & YILMAZ, Y. 1981. Tethyan evolution of Turkey: a plate tectonic approach. *Tectonophysics* **75**, 181–241.

ŞENGÖR, A.M.C., GÖRÜR, N. & ŞAROĞLU, F. 1985. Strike-slip faulting and related basin formation in zones of tectonic escape: Turkey as a case study. *In*: BIDDLE, K. & CHRISTIE-BLICK, N. (eds), *Strike-slip Deformation, Basin Formation and Sedimentation.* Society of Economic Paleontologists and Mineralogists, Special Publication **37**, 227–264.

ŞENGÖR, A.M.C., SATIR, M. & AKKÖK, R. 1984. Timing of tectonic events in the Menderes Massif, western Turkey: implications for tectonic evolution and evidence for Pan-African basement in Turkey. *Tectonics* **3**, 693–707.

SEYİTOĞLU, G. & SCOTT, B.C. 1991. Late Cenozoic crustal extension and basin formation in west Turkey. *Geological Magazine* **128**, 155–166.

SEYİTOĞLU, G. & SCOTT, B.C. 1992. The age of the Büyük Menderes graben (west Turkey) and its tectonic implications. *Geological Magazine* **129**, 239–242.

SEYİTOĞLU, G., TEKELİ, O., ÇEMEN, İ., ŞEN, Ş. & IŞIK, V. 2002. The role of the flexural rotation/rolling hinge model in the tectonic evolution of the Alaşehir graben, western Turkey. *Geological Magazine* **139**, 15–26.

ŞİMŞEK, Ş. 1997. Geochemical potential in Northwestern Turkey. In: SCHINDLER, C. & FISTER, M.P. (eds), Active Tectonics of Northwestern Anatolia - The Marmara Poly-Project, Vdf Hochschulverlag A Gander ETH Zürih, 111-123.

SÖZBİLİR, H. 2001. Geometry of macroscopic structures with their relations to the extensional tectonics: field evidence from the Gediz detachment, western Turkey. *Turkish Journal of Earth Sciences* **10**, 51–67.

SÖZBİLİR, H. 2002. Geometry and origin of folding in the Neogene sediments of the Gediz graben, western Anatolia, Turkey. *Geodinamica Acta* **15**, 277–288.

STEFANSSON, V. & STEINGRIMSSON, B. 1981. *Geothermal Logging I: An Introduction to Techniques and Interpretation* (2nd Edition). Reykjavik, National Energy Authority Report OS-80017/JHD-09.

TARCAN, G. 1995. *Hydrogeological Study of the Turgutlu Hot Springs.* PhD Thesis, Dokuz Eylül Üniversity Graduate School of Natural and Applied Sciences, İzmir, Turkey [unpublished].

VENGOSH, A., HELVACI, C. & KARAMANDERESİ, İ.H. 2002. Geochemical constraints for the origin of thermal waters from western Turkey. *Applied Geochemistry* **17**, 163–183.

VERGE, N.J. 1995. Oligo-Miocene extensional exhumation of the Menderes Massif, western Anatolia. *Terra Abstracts* **7**, p. 117.

WHITNEY, D.L. & BOZKURT, E. 2002. Metamorphic history of the southern Menderes Massif, western Turkey. *Geological Society of America Bulletin* **114**, 829–838.

YILMAZ, Y. 1997. Geology of western Anatolia. *In*: SCHINDLER, C. & FISTER, M.P. (eds), *Active Tectonics of Northwestern Anatolia-The Marmara Poly-Project.* Vdf Hochschulverlag A Gander ETH Zürih, 31–53.

YILMAZ, Y. & KARACIK, Z. 2001. Geology of the northern side of the Gulf of Edremit and its tectonic significance for the development of the Aegean grabens. *Geodinamica Acta* **14**, 31–40.

YILMAZ, Y., GENÇ, S.C., GÜRER, O.F., BOZCU, M., YILMAZ, K., KARACIK, Z., ALTUNKAYNAK, Ş. & ELMAS, A. 2000. When did the western Anatolian grabens begin to develop? *In*: BOZKURT, E., WINCHESTER J.A. & PIPER, J.D.A. (eds), *Tectonics and Magmatism in Turkey and the Surrounding Area.* Geological Society, London, Special Publications **173**, 353–384.

Received 11 March 2002; revised typescript accepted 02 April 2003